Replies document for reviews of:

The substructure of extremely hot summers in the Northern Hemisphere

Matthias Röthlisberger[1], Michael Sprenger[1], Emmanouil Flaounas[1], Urs Beyerle[1] and Heini Wernli[1]

[1]Institute for Atmospheric and Climate Science, ETH Zürich, Zürich, Switzerland

Corresponding author address:

Matthias Röthlisberger

Institute for Atmospheric and Climate Science,

ETH Zürich, Zürich, Switzerland

E-mail: matthias.roethlisberger@env.ethz.ch

General comments to the Reviewers

We would like to thank both reviewers for their thoughtful and overall encouraging reviews. The reviews were particularly useful for identifying weaknesses in the presentation of the material, but also helped to sharpen our own view of the value of our key results. Major changes that we made to the manuscript include the following: Both reviewers requested the novelties and key insights of this study to be presented more clearly and to account for these comments, we substantially re-worded Section 4. Moreover, we repeated all our analyses after removing a linear trend from all JJA T2m data at each grid point in both data sets, which meant that we also had to redraw all our figures. Note, however, that none of our original conclusions were altered by this detrending. Line numbers mentioned in in this document refer to line numbers in the revised manuscript, unless stated otherwise. Reviewer comments are included below in black font colour and our replies in blue.

Reviewer 1

This manuscript investigates Northern Hemisphere extreme hot summer seasons from a statistical point of view. The topic is relevant, because hot summers have societal impact and are going to become more frequent due to anthropogenic climate change. The paper focuses on the entire 3-month summer season rather than addressing individual heat waves (which have been studied before quite extensively). The method involves a novel statistical analysis based on ranking the 92 days of a summer season according to their anomaly with respect to the corresponding climatology. The results indicate that hot summers in different areas on the Northern Hemisphere may have different substructure: in some regions a summer season tends to be hot because the hottest tercile is anomalously hot, while in other regions the summer season tends to be hot because the coldest tercile is anomalously hot. In addition, it is shown that the Community Earth System Model (CESM) is able to broadly represent such regional differences. The regional differences are made plausible by studying a few cases/locations. I think these are interesting results. In addition, the paper is very well written. I have a few specific comments below which may help to produce a final version.

Comments:

Major:

1. My only general comment is the following. I found that the statistical method is well described and sounds very interesting, and while reading I was eagerly awaiting the discussion of possible physical causes. But then (reading that section) I was somewhat

disappointed. For instance, the shift in the onset of the Indian monsoon obviously explains the behavior found in the statistical analysis; actually, the explanation is so obvious that in retrospect the statistical analysis almost appears as an artifact. Let me grossly exaggerate to make my point clear: if you have a very simple phenomenon and apply a rather complex or strange analysis to it, you are likely to find a complex or strange result, but the complexity or strangeness of the result in this case would be mostly a feature of the analysis and not a feature of nature. Having said this, I still believe that the analysis is worth doing, and you do it very well.

We agree with the reviewer insofar as in some regions, the physical causes of extreme summers (and their substructure) are very easily understood. However, we do not believe that this jeopardizes the value of the results and novel insights presented in this study. Therefore, we understand this reviewer comment as a call for more clearly highlighting the novel insights derived from this study.

There are four main results of this study that could not have been achieved without developing and applying our novel seasonal anomaly decomposition. First, for each season and grid point, it allows to exactly quantify how much each rank day contributes to the seasonal anomaly or, similarly, how anomalous each rank day was. The key point here is that these results are quantitative and straight forward to understand. For example, our method allows to make statements like: the hottest 30 days of the 2010 summer at the grid point 35°E/58°N were each at least 4 K hotter than their respective rank day mean (i.e., their climatological value, Fig 4e). We expect such local quantitative statements to be particularly relevant for impact studies, as, e.g., excess mortality, ecosystem damages and agricultural yield losses during a particular extreme season conceivably strongly depend on the particular substructure of the extreme season.

Second, our method allows to study the spatial variability in the extreme summer substructure and, furthermore, allows to make statements about the relevance of the coldest, middle and hottest third of extreme summers in a spatially aggregated sense. For example, even though European and US heat waves have been studied widely in the past, it simply has not been known so far that, e.g., in Nevada, the coldest third of the summer days contribute most to extreme summers, while the hottest third of summer days is most important over the UK. Furthermore, it is a novel insight from this study that almost everywhere in the Northern Hemisphere, the coldest third of the summer contributes substantially (>25%) to extreme summer temperature anomalies. The general relevance of unusually mild summer days for extreme summers is an important result, as it illustrates that we cannot understand extreme summers solely by studying heat waves. Rather, a complete picture of what generates extreme summers must include an understanding of processes operating on longer than synoptic time scales and how they organize different types of synoptic scale-flow features to both prevent cold summer days and foster heat waves.

Third, our study unravels that the mean extreme summer substructure (i.e., averaged over all extreme summers at a particular grid point) can be assessed qualitatively from the variance and skewness of the underlying T2m distribution. This is relevant because there is a large and robust body of literature that has studied the dynamical drivers of the shape of the T2m distribution. Thus, at least qualitatively, the arguments put forward in these studies to explain the T2m distribution shape can also be used to explain the mean extreme summer substructure.

Fourth, we demonstrate that a state-of-the-art climate model (i.e., the CESM1 model) largely reproduces the observed extreme summer substructures. This result testifies to the model's ability to correctly reproduce the dynamical drivers of extreme summers and will be particularly relevant for subsequent studies on extreme summers (and their substructures) in a changing climate.

All of these four points are now made even more explicit in Section 4 (Summary and concluding remarks), in particular on lines 422-436:

"Furthermore, a key finding of this study is that the mean extreme summer substructure is consistent with the shape of the underlying local T2m distribution. The extreme summer substructure is largely determined by which of the 92 JJA rank days are most variable (i.e., the rank day variability pattern), which is qualitatively related to the skewness of the T2m distribution. Simply speaking, in regions where the coldest days of the summer are most variable (i.e., negatively skewed T2m distribution), extreme summers occur when the coldest days of the summer are unusually hot, and, analogously, for the case where hottest days vary the most (i.e., positively skewed T2m distribution). This finding is relevant for two reasons. Firstly, it constrains what kind of extreme summer substructures can locally be expected, in particular in regions with strongly skewed daily temperature distributions. For example, extreme summers arising primarily from extremely hot summer days (i.e., heat waves) are unlikely to occur in regions with strongly negatively skewed temperature distributions. Secondly, some individual extreme summers such as the 2010 summer at the grid point at 35°E/58°N featured clear temperature regime shifts, with rank day anomalies far outside of what could be expected from their climatological variability (e.g., almost twice as large as the second large anomalies for the same ranks during the 2010 summer at 35°E/58°N). The general consistency between the mean extreme summer substructure and the skewness of the underlying T2m distribution illustrates that such regime shifts in the temperature variability during extreme summers are the exception rather than the norm."

And on lines 481-509: "A further key result of this study is that in most places, the cool summer days contribute substantially to extreme summer T2m anomalies [more than 25% over 83% (86%) of the Northern Hemisphere land area in ERAI (CESM)]. In fact, Fig. 5 reveals that for ERA-Interim (CESM) in 46% (49%) of the Northern Hemisphere land area, the coldest third of the summer contributes more to the extreme summer anomaly (XA) than the hottest third. Thus, large positive seasonal temperature anomalies (i.e. extreme summers as opposed to individual heat waves), cannot be understood and explained by only considering the physical drivers of heat waves. Rather, the processes which suppress the occurrence of cold summer days must also be considered. Yet, these processes are so far virtually unexplored and thus possibly yield an untapped potential for improving our understanding of extreme summers. However, as illustrated by the example of extreme summers in the western US, the processes that suppress the occurrence of cold summer days sometimes seem rather intangible, as they do not necessarily manifest themselves in the occurrence of an unusual flow pattern, but rather in the non-occurrence of the particular flow that typically produces the coldest summer days.

This study has illustrated that extreme summers across the Northern Hemisphere have distinct substructures, which result directly from the physical causes of the extreme summers. However, the concept of the extreme season substructure has applications beyond what has been presented in this study and thus calls for subsequent studies. Firstly, the presented analyses could be extended to the Southern Hemisphere and other seasons and variables. (The application of the technique is most promising for variables that are potentially unbound and variable on both ends, i.e., not for a positive definite variable like precipitation.) Secondly, the concept of a "season substructure" can be relevant for field campaigns, as the representativeness of the campaigns' measurements depends on how representative the time period of the campaign was (Wernli et al., 2010). Thirdly, extreme summers with distinct substructures conceivably have different societal effects and thus future research should assess whether or not and where the extreme summer substructure is affected by climate change. The results of this study suggest that the CESM is a suitable tool for this task, as it is largely able to reproduce the observed (ERA-Interim) extreme summer substructure in the current climate. However, some of the extreme summers observed within the last 40 years appear to be outside of the spectrum of 700 years of CESM. Hence, while CESM is able to reproduce the local extreme summer substructures, it may not be able to reproduce the most extreme summers that are physically possible in some regions. Clearly, this finding requires detailed and critical further investigation. Finally, changes in the extreme summer substructure with climate change must be related to changes in the physical causes of extreme summers, as a uniform warming would not affect the local rank day variability pattern. Therefore, contrasting extreme summer substructures in present and future climate simulations might also help to identify regions where the physical causes of extreme summers are altered by climate change."

Minor:

1. Line 68: Can you give here an example, too?! You could, for instance, mention Nevada (USA) and say that this will be discussed later.

   We prefer not to give an additional example here for two reasons. First, we call these other possibilities "plausible", as at this stage in the study it is not yet clear whether or not they at all occur. Second, we discuss distinct substructures in much detail on lines 181-231 and would not like to make reference to these examples (which are "results" of this study) already in the introduction.

2. Line 96: Do you really "illustrate physical causes"? I feel that you, rather, aim to "uncover the underlying physical causes for the different summer substructures".

We believe that we indeed “illustrate physical causes”, but the second part of the sentence, “in selected regions”, is just as important. The phrasing suggested by the reviewer appears to imply that particular extreme summer substructures have particular physical causes, regardless of where on the globe they occur. Given that similar extreme summer substructures can be found e.g., over the northern Sahel region and the high Arctic, we should have stated more clearly that of course distinct physical causes might lead to one and the same extreme summer substructure, provided they occur in different regions.

To account for this comment, lines 474-479 now read: “Clearly, distinct physical causes might lead to similar extreme summer substructures, in particular when comparing regions that are far apart (e.g., the northern Sahel region and the high Arctic, Fig. 5). However, similar extreme summer substructures in neighboring regions conceivably also point to similar physical causes of extreme summers (e.g., the Asian Monsoon region). Therefore, the extreme summer substructure is a helpful tool for discriminating between neighboring regions with distinct physical causes of extreme summers and might also be helpful for identifying coherent regions with similar physical causes of extreme summers.”

3. Beginning of section 2.3: At this point I thought your analysis implies some spatial averaging, e.g., a summer season in Switzerland. Only later it becomes clear that this analysis is done grid-point wise. It would help me if you can say this rather early in the text.
   We have added on line 130 “Furthermore, bear in mind that all these quantities are calculated at each grid point individually.”.

4. Line 134: You could add that D = 92 = the number of days in the summer season.
   This information is already provided on line 125. We therefore prefer not repeat it on original line 134.

5. Line 238: "most regions"? 46% of the NH land area is less than half of the land area, so in what sense is this "most regions"? Did I get something wrong here? The same remark applies to the summary section (line 448).

The original sentence read: “Overall, Fig. 5c clearly demonstrates that the coldest third of all summer days contributes a substantial fraction to XA^{ERAI} in most regions.”. Hence, “most regions” refers to “the regions where the coldest third of all summer days contributes a substantial fraction to XA^{ERAI}”. The 46% on the other hand, refer to regions where the contribution from the coldest third exceeds the contribution from the hottest third. The question is thus what we are willing to call “a substantial fraction”. Figure 5c shows that XF_{cold}^{ERAI} is less than 25% only in very few regions, which is why we stated that almost everywhere it is “substantial”.

To clarify this point we have rephrased this sentence (now lines 250-251) to: “Overall, Fig. 5c clearly demonstrates that the coldest third of all summer days contributes a substantial fraction to XA^{ERAI} in most regions [more than 25% over 83% of the Northern Hemisphere land area in ERAI]”

6. Line 273: I wonder to what extent this "result" is more or less trivial: To the extent that a particular tercile of the distribution is much more variable than the other two, does this not imply by necessity that an anomalous season must be due to this tercile being anomalous? If this is so (i.e., more or less trivial), you should say this; if I am wrong and this is not trivial, it would help (me, but possibly other readers as well) to explain why it is not trivial. This remark applies equally to the conclusion section (line 407) and the abstract (line 26).

Indeed, in retrospect, this result is rather easily understood, and thus plausible. However, it is nevertheless certainly relevant, at least for two reasons. First, it is not a priori clear that the climatologically most variable tercile must contribute most to extreme seasons, as also some kind of temperature regime shifts could occur during the most extreme seasons. Such a regime shift can be observed during the 2010 summer at the grid point 35°E/58°N, during which the hottest 30 days exhibited rank day anomalies that were roughly twice as large as during the second most extreme summer (Fig. 3e) and thus clearly showed a different behaviour than in the climatology. The result referred to by the reviewer shows that such regime shifts do not generally occur during extreme summers.

Second, it is not so much the result itself but rather its implications that are non-trivial. The fact that the extreme summer substructure is consistent with the underlying T2m distribution constrains the possible extreme summer substructures. For example, in a region with strongly negatively skewed temperature distribution, extreme summers are very unlikely to arise from typical "heat waves", but rather must arise from processes that supress cool summer days. However, those processes have hitherto not been studied extensively. We are not aware of any previous study making this point and therefore find it novel and relevant.

We now mention the relevance of this result explicitly on lines 423-436: "Furthermore, a key finding of this study is that the mean extreme summer substructure (i.e., the average substructure of all extreme summers at a particular grid point) is consistent with the shape of the underlying local T2m distribution. The mean extreme summer substructure is largely determined by which of the 92 JJA rank days are most variable (i.e., the rank day variability pattern), which is qualitatively related to the skewness of the T2m distribution. Simply speaking, in regions where the coldest days of the summer are most variable (i.e., negatively skewed T2m distribution), extreme summers occur when the coldest days of the summer are unusually hot, and analogously for the case where hottest days vary the most (i.e., positively skewed T2m distribution). This finding is relevant for two reasons. Firstly, it constrains what kind of extreme summer substructures can locally be expected, in particular in regions with strongly skewed daily temperature distributions. For example, extreme summers arising primarily from extremely hot summer days (i.e., heat waves) are unlikely to occur in regions with strongly negatively skewed temperature distributions. Secondly, some individual extreme summers such as the 2010 summer at the grid point at 35°E/58°N featured clear temperature regime shifts, with rank day anomalies far outside of what could be expected from their climatological variability (e.g., twice as large as the second large anomalies for the same ranks during the 2010 summer at 35°E/58°N). The consistency between the mean extreme summer substructure and the skewness of the (full) T2m distribution illustrates that such regime shifts in the temperature variability during extreme summers are the exception rather than the norm."

7. Line 284: "closely"— really? There is quite some resemblance, but I would not call it "close".

   We deleted "closely".

8. Line 364: Is this really a "breaking" trough? In my eyes this is a large (nonlinear) trough, but not quite breaking (yet).
   Following McIntyre & Palmer (1983) and Martius, Schwierz, & Sprenger (2007) we use “breaking trough” synonymously with “nonlinear trough”. It is important to bear in mind that this is a composite trough. Hence, if the composite trough (composited over 100 days) already features meridionally overturning of PV contours, we do feel confident to call it a breaking trough.

9. Line 405: Can you speculate why in some areas there is no good correspondence between CESM and ERA-Interim?
   The reviewer raises a very interesting question, which in our opinion might warrant a subsequent study. However, as the reviewer points out quite rightly, based on the presented results we could only speculate about why CESM and ERAI extreme summer substructures disagree in some regions. We are concerned that speculation about this point might lead to more confusion than clarity and therefore refrain from doing so.

10. Line 302: Should it not read V Fcold and V Fhot?!
    Yes, indeed, many thanks for spotting this error! We have changed this according to the reviewer comment.

11. Line 588: Is "Earth’s Futur." the title of the journal?
    Yes, the title of the journal is “Earth’s Future”, which is abbreviated in the WCD citation style to “Earth’s Futur.”. The paper can be accessed under:
    https://agupubs.onlinelibrary.wiley.com/doi/full/10.1029/2019EF001189

Reviewer 2

Summary: In this paper, the authors introduce the method of calculating rank day anomalies for each summer in order to characterize the distribution of temperatures during extreme summers. The method, as I understand it, is to sort the 92 daily mean temperature values at each location and then calculate the average at each rank. Then for each summer, the deviation from this climatological mean is taken. They find that in the arctic, extreme summers occur when cold days are warmer than usual and in India, the hottest days drive the anomalously extreme summers. A point that I think is particularly important that is made somewhat in passing is that the characteristics of the extreme summers are consistent with the characteristics of the underlying temperature distributions—there is no obvious regime shift or equivalent for the hottest summers. From this perspective, I think this is a useful tool to verify that we can understand extreme seasons by understanding the underlying temperature distributions. Overall, I find this study to be worthwhile, but a bit confusing. As the authors state, this is a novel method for looking at extreme summers. They do not spend much time justifying the introduction of such a method, and the advantages it has over examining the local temperature distributions themselves or over methods such as looking at compound heatwaves (Baldwin et al. 2019). Indeed, one of my main takeaway messages from this paper was that extreme summers can be relatively well described by understanding the variance and skewness of the underlying temperature distribution (more below). This method proved that particular point quite nicely. If there are other advantages or conclusions that can be drawn uniquely from these metrics, the authors should highlight them. I believe this paper will be suitable for publication after it addresses the following concerns:

Major:

1. As mentioned above, what is the advantage of this method over more typical examinations of temperature distributions? How does the calculation of RDA differ from quantile analysis? How does the comparison of the contributions of the top 33% and the bottom 33% differ from examining skewness? How does the spatial pattern of XA compare to the spatial pattern of temperature variance? I have included plots based on the ERA-I data I had handy (850 hPa, 1980-2014, 4xdaily), but I think the inclusion of ERA-I surface temperature variance and skewness plots is essential. The comparison with Loikith et al. 2018 is pretty impossible given the size of the panels in their Fig 4.

   There are several ways in which our method differs from the standard characterizations of the T2m distribution listed by the reviewer and which make our method a valuable tool that is complementary to standard methods.

   A first difference lies in the purpose of the method we developed. The novelty of this study is that it assesses how entire summer seasons become extreme from a statistical (and partly dynamical) point of view. This research question is certainly relevant as recent extreme summers had large societal impacts (going beyond the impacts of individual heat waves) and which therefore call for a better understanding of extreme summer seasons overall. In the process of addressing our research question we learned that the mean extreme summer substructure at a particular grid point can be inferred qualitatively from the skewness of the underlying daily temperature distribution. As the reviewer quite rightly noticed, this is a very important result of this study which could not have been anticipated beforehand. However, for any study, the choice of method is driven by the purpose of the study and not by its final results. Therefore, the quantities and methods we work with ($RDA, XA,$ etc.) are natural and meaningful choices for addressing our research question, and their development and application was imperative for arriving at the understanding of extreme summers that we now have.

Second, our method does not only allow to analyse the mean behaviour of extreme seasons at a particular grid point (i.e., averaged over all extreme seasons at a particular grid point) but can also characterize individual extreme seasons. Figures 4b,c show two examples of distinct extreme summer substructures occurring at one particular grid point. In such regions, the ability to characterize individual extreme seasons is certainly an advantage over simply characterizing the mean extreme season. Furthermore, the degree to which different extreme summers at a particular grid point resemble each other cannot be inferred from considering skewness and variance of a particular T2m distribution, but this information is readily available after employing the method developed here. For this particular purpose, quantile analysis would certainly be a valid alternative (which we actually tested in an earlier stage of this work). However, the method developed in this study allows for an exact decomposition of the seasonal anomalies, which does not rely on any quantile function and which we therefore consider to be more elegant.

Third, we believe that the quantitative results of our seasonal anomaly decomposition are particularly straightforward to understand. For example, Fig. 4e reveals that at 35°E/58°N the hottest 30 days of the 2010 summer were each at least 4 K warmer than the climatological values of the 30 hottest days, which for some ranks is more than 2 K more than the second hottest summer. Moreover, at the grid point in India, the hottest third of the summer 2005 contributed 95% of the seasonal mean anomaly. Finally, we show that over 46% of the land mass, the coldest third of extreme summers contributes more to the extreme summer anomaly than the hottest third. We do not see how such exact quantitative statements on the substructure of extreme summers could be achieved based on the analyses suggested by the reviewer. However, we strongly believe that such exact quantitative statements are valuable and convey particular characteristics of extreme summers in a very intuitive way.

In order to account for this comment, we have substantially reworded and extended the summary and concluding remarks (Section 4, lines 403-509) and moreover included Fig. S1 which shows the skewness of the daily T2m distribution in ERAI (Fig. S1 is also included at the end of this document). Furthermore, we now clearly state whether we discuss mean extreme summer substructures (i.e., averaged over all extreme summers at a particular grid point) or the substructure of a particular summer.

2. The authors need to better justify not somehow accounting for the trend in summertime temperatures in ERA-I (or better yet, they need to account for the trend). The current justification, i.e., "as we are interested in extreme summers exhibiting the largest absolute T2m anomalies and not the largest T2m anomalies relative to a longterm trend" does not make sense in the context of the later discussion. The analysis as currently presented naturally conflates factors associated with global warming with the dynamics associated with internal modes of climate variability. e.g. The point in Nevada has 2016, 2017, and 2018 all included in its five most "extreme" summers. The earliest "extreme" summer there is 2007. Surely, then the signal in RDA is one of global warming. And indeed, if we compare this to the results of McKinnon et al. (2016a) Figure 4, we see a warming of the whole distribution and the largest warming in the bottom quantiles. This then seems to be an examination of the forced response rather than internal variability. Meanwhile the authors argue, quite convincingly, that the extreme summers in India are related to the timing of the monsoon onset, a signal too strong to be dominated by global warming.

We agree with the reviewer on this point. The intention of this study was to understand how the most extreme (i.e., often recent) summers became so extreme. However, the reviewer is right, not detrending the T2m data might obscure the causes of extreme summers arising from internal variability.

To account for this comment, all analyses have been repeated after removing a linear trend from JJA data, separately at each grid point and in both data sets. The new Figs.

2, 8 and 9 have been produced with non-detrended data, as for these figures absolute values of T2m are either more intuitively understood (Figs. 2 and 8) or the absolute value of T2m is relevant (Fig. 9). However, also for these Figures, extreme seasons have been identified based on the detrended data.

None of our conclusions are altered by this detrending. However, some of the archetypical extreme seasons that we used to illustrate archetypical extreme seasons in the original Section 3.2 no longer appear as extreme seasons. Therefore, in Figs. 3d,e and 4d,e we now show results for the grid points closest to Paris (2°E/49°N) and at 35°E/58°N). Note further that for the Nevada grid point the rank day variability pattern remains almost unchanged, even though the extreme seasons are now more evenly spread throughout the ERAI period.

3. "Substructure" is not really an appropriate representation of what is studied in this paper. This study is not detailing the relative timing and duration of heatwaves—indeed all temporal ordering is lost in the novel method introduced here. Substructure as I would typically understand it is considered in Fig. 1 and Fig. 8 only. This isn't such a major point about the importance of the paper, but it will require some thought as to a more appropriate term and then significant rewriting.

We disagree with the reviewer here but nevertheless appreciate this comment as it points to a possible source of confusion that we wish to avoid in the revised manuscript. To our knowledge, the term "season substructure" is not (yet) a widely used term in atmospheric sciences. In particular, "season substructure" does not necessarily need to have some kind of temporal meaning. Therefore, we allow ourselves to use this term in a way that does not relate to temporal ordering but that we nevertheless do find appropriate and meaningful.

Arguably, the term "season substructure" implies some kind of disaggregation of a season into its sub-parts. Consequently, studying the "season substructure" means studying particular aspects of these sub-parts. Admittedly, one such disaggregation could be temporal and in this case, studying the season substructure would indeed mean studying, e.g., the early, middle and late parts of the season (or any other consecutive time periods during the season, such as individual heat waves). However, equally well this disaggregation could be with regard to temperature or any other variable. In this case, studying the substructure of a season means studying particular aspects of the cold, middle and warm parts of this season. This is exactly how we use this term in this study and we therefore think that it indeed is appropriate.

However, we have realized that in Fig. 1 and on original lines 60-69 we unintentionally implied a disaggregation over time, which of course was misleading the reader. We have therefore adjusted the schematic in Fig. 1 and rewritten the original lines 60-69 (now lines 60-69) to: "Like any other summer, an extreme summer will inevitably contain cooler and hotter days, which constitute the upper and lower parts of the T2m distribution during that summer. However, it is currently not known which part of the T2m distribution is particularly anomalous during an extreme summer. Thus, extreme summers with distinct "substructures" might occur, some of which are schematically illustrated in Fig. 1. For example, a summer might be an extreme summer because the hottest days of the season are particularly anomalous, with the remainder of the summer days being only moderately warmer than or even close to climatology. Such an extreme summer substructure was observed in large parts of Europe in the summer 2015, when the anomalies of the seasonal hottest days exceeded those of the seasonal mean by almost a factor of two (Dong et al., 2016). Hence, the hottest days of the 2015 summer contributed over proportionally to the seasonal mean anomaly. However, also other substructures are plausible: a suppression of cool summer days, a uniform shift in the entire summer temperature distribution or any combination of these three options.".

Other points:

1. The use of "d" in the equations in combination with the term "substructure" made me mistake "d" for day instead of rank. Consider a different variable name, perhaps? Or explicitly mention that ordering is lost?

   We have rephrased the sentence on line 134, which now reads: "…T2m value with rank d in season k (i.e., the temporal ordering of the days is lost, see Fig. 2b)."

2. 144 rewrite for clarity. Perhaps just "allows assessment of"? Consider adding a specific example here.

   An example has been added on lines 146-148: "For example, if for a particular season k $SA_k = 1$ K and $RDA_{92,k} = 3$ K (i.e., the hottest day of season k is 3 K warmer than the respective rank day mean) this day contributed $3/92 = 0.0326$ K or 3.26% to the seasonal anomaly SA_k."

3. Consider mentioning which "third" is 30 days so that this calculation is perfectly reproducible

   Lines XY read: "The notation $[x]$ hereby stands for x rounded to the nearest integer. For computing contributions to SA_k from the middle and hottest thirds of the summer days ($SF_{middle,k}$ and $SF_{hot,k}$), the sum in Eq. (5) runs from $\left[\frac{D}{3}\right] + 1$ to $\left[D\,\frac{2}{3}\right]$ for $SF_{middle,k}$ and from $\left[D\,\frac{2}{3}\right] + 1$ to D for $SF_{hot,k}$." From this statement it is clear that the coldest "third" only contains 30 days.

4. 181 Normally -> normal

   Changed as requested by the reviewer.

5. Consider changing the figures so that it is easier to compare ERA-I and CESM. E.g. put Fig 3a and 4 a together.

   We have considered this option but we find it more intuitive to present the anomalies XA^M alongside with their respective decompositions and therefore chose to stick to the original figure layout for Figs. 3 and 4.

6. Paragraph beginning l. 243: the quantitative spatial correlation value would be helpful here.

   We are not entirely sure what measure of spatial correlation the reviewer has in mind exactly. We prefer to leave this passage as it was originally.

7. Fig. 6: The yellow contours are really difficult to read. Consider having thin dotted lines for continents so that you could use thicker black lines in place of the yellow? Or some other change to make this more readable. Magenta might be better than yellow.

   We have changed the contour color to green and adjusted the contour levels to make them more readable.

8. l. 359 normal

   Changed as requested.

9. Fig. 9: Label lines within the panel b

   Labels have been added in panel b.

10. Analysis of Nevada. Consider work by McKinnon et al. (2016b), which is primarily looking at Eastern US, but their conclusions still seem relevant.

    The work of McKinnon et al. (2016b) is certainly most interesting, in particular if one aimed at predicting the substructure of summer with a seasonal forecasting system. For the Nevada grid point, however, we do not see how exactly the work of McKinnon et al. (2016b) relates to our analysis, since their focus is primarily on the Eastern US and on predicting hot days from a particular tropical SST pattern.

11. l. 381 Why … the troughs associated with cold anomalies (black contours in 10a) did not occur…

    The "right phasing" seems crucial to us here and there might well have been troughs with associated cold anomalies during these extreme summers, just not over the Nevada region. Therefore, we prefer our original formulation here.

12. l. 388 It seems like the goal (c.f. Hoskins and Woollings 2015) is to explain the full shape of the temperature PDF, since extreme summers seem consistent with the underlying distribution. But you are correct that a combined approach is necessary for that as well. So maybe just add "… to fully reveal the physical causes of the full shape of the temperature distribution, including extreme summers" or something along those lines?

    The reviewer comment is correct insofar as "fully revealing the physically causes of the full temperature distribution" would also help to understand the physical causes of extreme summers. This paper, however, focusses first and foremost on extreme summers and therefore we prefer to stick to our original wording.

13. Paragraph beginning l. 406: This seems like perhaps the major conclusion of this work. Emphasize this more at the beginning.

    We now emphasize this result much more in Section 4.

14. l. 425 This phrasing is not appropriate. “Often” cannot be determined from these three case studies, and one of the three case studies (US) is in fact a clear case of temperature advection’s importance due to an anomalously zonal jet stream.

    We have changed the wording to (now line 450-452) “However, three case studies illustrate that the extreme summer substructure cannot always be explained by temperature advection alone.”

15. Paragraph beginning l. 436: This is completely consistent with the eddy advection argument of Garfinkel and Harnik 2017, Tamarin-Brodsky et al. 2019, and Linz et al. 2018.

    We agree. Reference is now made to all three studies on lines 468-469: “This result is consistent with previous work on physical causes of non-Gaussian temperature distributions (Garfinkel and Harnik, 2017; Linz et al., 2018; Tamarin-Brodsky et al., 2019), as it highlights the role of temperature advection by transient waves in generating a non-uniform rank day variability pattern, or similarly, a skewed T2m distribution.”

16. l. 443 New paragraph

    Changed as requested.

17. l. 445 Not convinced of this (esp. the coherent regions aspect, since mostly this has looked at individual points) by this particular study.

    We have rephrased this paragraph in order to be more precise about how the extreme summer substructure might help to delineate coherent regions with similar drivers of extreme summers.

    Lines 474-479 now read: “Clearly, distinct physical causes might lead to similar extreme summer substructures, in particular when comparing regions that are far apart (e.g., the northern Sahel region and the high Arctic, Fig. 5). However, similar extreme summer substructures in neighboring regions conceivably also point to similar physical causes of extreme summers (e.g., the Asian Monsoon region). Therefore, the extreme summer substructure is a helpful tool for discriminating between neighboring regions with distinct physical causes of extreme summers and might also be helpful for identifying coherent regions with similar physical causes of extreme summers.”

18. l. 455 A more zonally symmetric/less wavy flow is still a pattern, so this phrasing doesn't really make sense.

It is true that a less wavy flow is still a flow pattern but it is not "the particular flow pattern necessary to produce cold summer days". The point here really is to say that for producing abnormally mild coldest summer days no special flow pattern is required. Rather, the particular pattern that usually generates the coldest summer days just does not occur.

To clarify this point we have rephrased lines 488-491 to: "However, as illustrated by the example of extreme summers in the western US, the processes that suppress the occurrence of cold summer days sometimes seem rather intangible, as they do not necessarily manifest themselves in the occurrence of an unusual flow pattern, but rather in the non-occurrence of the particular flow that typically produces the coldest summer days.".

Martius, O., Schwierz, C., & Sprenger, M. (2007). Dynamical tropopause variability and potential vorticity streamers in the Northern Hemisphere — A climatological analysis. *Adv. Atmos. Sci.*, *25*(3), 367–380. https://doi.org/10.1007/s00376-008-0367-z

McIntyre, M. E., & Palmer, T. N. (1983). Breaking planetary waves in the stratosphere. *Nature*, *305*(5935), 593–600. https://doi.org/10.1038/305593a0

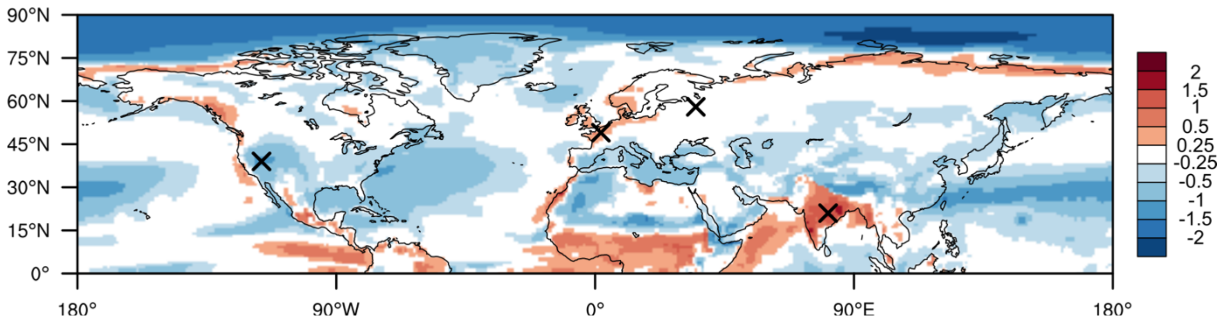

Figure S1. Skewness of daily T2m in ERA-Interim. Black crosses as in Fig. 3a.

The substructure of extremely hot summers in the Northern Hemisphere

Matthias Röthlisberger[1], Michael Sprenger[1], Emmanouil Flaounas[1], Urs Beyerle[1] and Heini Wernli[1]

[1]Institute for Atmospheric and Climate Science, ETH Zürich, Zürich, Switzerland

Correspondence to: Matthias Röthlisberger (matthias.roethlisberger@env.ethz.ch)

Abstract. In the last decades, extremely hot summers (hereafter extreme summers) have challenged societies worldwide through their adverse ecological, economic and public health effects. In this study, extreme summers are identified at all grid points in the Northern Hemisphere in the upper tail of the July–August (JJA) seasonal mean 2-meter temperature (T2m) distribution, separately in ERA-Interim reanalyses and in 700 simulated years with the Community Earth System Model (CESM) large ensemble for present-day climate conditions. A novel approach is introduced to characterize the substructure of extreme summers, i.e., to elucidate whether an extreme summer is mainly the result of the warmest days being anomalously hot, or of the coldest days being anomalously mild, or of a general shift towards warmer temperatures on all days of the season. Such a statistical characterization can be obtained from considering so-called rank day anomalies for each extreme summer, that is, by sorting the 92 daily mean T2m values of an extreme summer and by calculating, for every rank, the deviation from the climatological mean rank value of T2m.

Applying this method in the entire Northern Hemisphere reveals spatially strongly varying extreme summer substructures, which agree remarkably well in the reanalysis and climate model data sets. For example, in eastern India the hottest 30 days of an extreme summer contribute more than 65% to the total extreme summer T2m anomaly, while the colder days are close to climatology. In the high Arctic, however, extreme summers occur when the coldest 30 days are substantially warmer than climatology. Furthermore, in roughly half of the Northern Hemisphere land area, the coldest third of summer days contribute more to extreme summers than the hottest third, which highlights that milder than normal coldest summer days are a key ingredient of many extreme summers. In certain regions, e.g., over western Europe and western Russia, the substructure of different extreme summers shows large variability and no common characteristic substructure emerges. Furthermore, we show that the typical extreme summer substructure in a certain region is directly related to the region's overall T2m rank day variability pattern. This indicates that in regions where the warmest summer days vary particularly strongly from one year to the other, these warmest days are also particularly anomalous in extreme summers (and analogously for regions where variability is largest for the coldest days). Finally, for three selected regions, thermodynamic and dynamical causes of extreme summer substructures are briefly discussed, indicating that, for instance, the onset of monsoons, physical boundaries like the sea ice edge, or the frequency of occurrence of Rossby wave breaking, strongly determine the substructure of extreme summers in certain regions.

hat gelöscht: 70

1 Introduction

During the last decades, numerous high-impact hot temperature extremes occurred on approximately seasonal time scales, including the extremely hot European summer in 2003 (Fink et al., 2004; Schär and Jendritzky, 2004), the 2010 Russian heat wave (Barriopedro et al., 2011), the hot and dry summer 2015 in Europe (Dong et al., 2016; Hoy et al., 2017; Orth et al., 2016), the hot and humid summer 2015 in western India and Pakistan (Wehner et al., 2016), and the concurrent heat waves across the Northern Hemisphere in the summer 2018 (Vogel et al., 2019). It is well known that individual heat waves on time scales of up to a few weeks cause societal challenges, for example serious public health issues (e.g., Fouillet et al., 2006). However, the large socio-economic and ecological impacts of the seasonal events listed above (e.g., Ciais et al., 2005; Buras et al., 2019) illustrated that many economic sectors such as agriculture, tourism and re-insurance are particularly susceptible to temperature extremes on seasonal (as opposed to synoptic) time scales. Therefore, understanding the statistical properties of entire extremely hot summers (hereafter referred to as “extreme summers”) as well as their physical causes is a research topic of high societal relevance.

The concept of an extreme summer [as a particular type of an “extreme season”, cf. Wernli et al. (in prep.)] is closely related to the concept of a heat wave, even though there are important differences. An individual heat wave is commonly understood to be a single, quasi-continuous episode of abnormally hot surface weather with a duration ranging from days to weeks (Russo et al., 2015; Zschenderlein et al., 2019). Heat waves are thus strongly influenced by individual synoptic flow features such as atmospheric blocks (Brunner et al., 2017; Pfahl and Wernli, 2012; Röthlisberger and Martius, 2019; Zschenderlein et al., 2019), stationary ridges (Sousa et al., 2018) or recurrent Rossby wave patterns (Röthlisberger et al., 2019). In contrast, extreme summers have a fixed duration (of three months), which is beyond the time scale of these synoptic flow features. Consequently, extreme summers require a temporal organization of the relevant synoptic flow features, which can occur either “by chance” (internal atmospheric variability) or favored by more slowly varying processes. Possible candidates for the latter are soil moisture fluctuations (Fischer et al., 2007; Lorenz et al., 2010; Seneviratne et al., 2010), sea ice dynamics (Cohen et al., 2014) or large-scale modes of variability in the ocean and atmosphere (e.g., Schneidereit et al., 2012). Understanding how this temporal organization of weather within seasons occurs is challenging as it requires a seamless approach (Hoskins, 2013), which couples weather system dynamics to these more slower varying processes.

Like any other summer, an extreme summer will inevitably contain cooler and hotter days, which constitute the upper and lower parts of the T2m distribution during that summer. However it is currently not known which part of the T2m distribution is particularly anomalous during an extreme summer. Thus, extreme summers with distinct “substructures” might occur, some of which are schematically illustrated in Fig. 1. For example, a summer might be an extreme summer because the hottest days of the season are particularly anomalous, with the remainder of the summer days being only moderately warmer than or even close to climatology. Such an extreme summer substructure was observed in large parts of Europe in the summer 2015, when

Feldfunktion geändert

hat gelöscht: In contrast to individual heat waves,

hat gelöscht: extreme

hat gelöscht: s

hat gelöscht: may be composed of one or several hot periods

hat gelöscht: In some cases, an extreme summer may even contain rather cool periods separating individual heat waves.

hat gelöscht: exhibit distinct

the anomalies of the seasonal hottest days exceeded those of the seasonal mean by almost a factor of two (Dong et al., 2016). Hence the hottest days of the 2015 summer contributed over proportionally to the seasonal mean anomaly. However, also other substructures are plausible: a suppression of cool summer days, a uniform shift in the entire summer temperature distribution or any combination of these three options.

hat gelöscht: several episodes of hot but not extreme temperatures, perhaps even interrupted by fewer cool episodes,

hat gelöscht: or

Knowledge about the extreme summer substructure is relevant for at least two reasons. Firstly, the societal impact of an extreme summer featuring one (or several) periods of extremely hot temperatures (i.e., hottest summer days being hotter than normally) will likely differ from the societal impact of an extreme summer resulting primarily from a suppression of cool summer days (i.e., coldest summer days being milder than normally), or from an extreme summer characterized by a uniform shift in the entire temperature distribution (i.e., all summer days warmer than normally). Secondly, also the physical and meteorological causes of extreme summers with such distinct substructures conceivably differ. Thus, identifying the substructure of extreme summers is likely a starting point for understanding also their physical causes.

The purpose of this study is to characterize extreme summers statistically by quantifying their substructure. To do so, we define extreme summers in the upper tail of the June–August (JJA) mean two-meter temperature (T2m) distribution. Thereafter, the extreme summer substructure is assessed by decomposing the seasonal mean T2m anomaly of a particular extreme summer into the contributions from all rank days of that season (i.e., the contribution from the coldest day, the second coldest day etc.). This decomposition thus allows to quantify the contributions from all parts of the T2m distribution (e.g., the coldest, middle and hottest thirds of summer days) to the seasonal T2m anomaly of an extreme summer.

Here we use the ERA-Interim re-analysis data set to study the substructure of past extreme summers. However, extreme summers are by definition extremely rare events. Thus, in order to yield robust results, a climatological investigation of the extreme summer substructure requires much longer data records than provided by ERA-Interim or any other currently available high-quality re-analysis data set. We therefore complement ERA-Interim with a 700-year present day climate simulation (for details, see Sect. 2.2) to address the following research goals:

1. Propose and illustrate a simple method for decomposing at each grid point the seasonal mean temperature anomaly into its contributions from each rank day.
2. Use this decomposition to analyze the substructure of extreme summers separately at selected grid points.
3. Quantify and compare the spatial variability in extreme summer substructures in the Northern Hemisphere in both re-analysis and climate model data.
4. Illustrate physical causes of the observed (and simulated) extreme summer substructures in selected regions.

2 Data and Methods

2.1 ERA-Interim

We use ERA-Interim re-analysis data (Dee et al., 2011) covering the period 1979-2018. ERA-Interim is originally produced with a T255 spectral horizontal resolution and 60 hybrid σ-p levels in the vertical. We interpolated the data horizontally to a 1° by 1° grid and vertically to pressure and isentropic levels. The ERA-Interim data is provided at 6-hourly time intervals, in this study however, we aggregated all data to a daily temporal resolution. Besides the T2m fields, we also use potential vorticity (PV), total precipitation, 250 hPa meridional winds and sea ice concentration. Furthermore, we remove a (40-year) linear trend from all JJA T2m data at each grid point. Our analyses hereafter are based on the detrended data except for Figs. 2, 8 and 9, which are more easily understood based on the non-detrended data (Figs. 2 and 8) or where the absolute T2m values are important (Fig. 9).

hat gelöscht: we deliberately do not detrend the ERA-Interim T2m data as we are interested in extreme summers exhibiting the largest absolute T2m anomalies and not the largest T2m anomalies relative to a long-term trend.

2.2 CESM

Besides ERA-Interim, the Community Earth System Model version 1 (CESM, Hurrell et al., 2013) is used to perform present-day climate simulations using restart files from the CESM large ensemble project (CESM-LENS, Kay et al., 2015). We use atmospheric fields at daily temporal resolution, with a horizontal resolution of approximately 1° and 30 vertical levels. The original CESM-LENS data contains a 35-member ensemble of simulations started on 1 January 1920 and integrated forward in time until 2100. These 35 "macro ensemble" members were rerun for the period from 1 January 1990 to 31 December 1999 in order to obtain temporally high-resolution three-dimensional model output. To further increase the number of simulated JJA seasons, a "micro ensemble" with additional 35 members was branched off from member one of the macro ensemble, on 1 January 1980, by adding an $\mathcal{O}(10^{-13})$ perturbation to the initial atmospheric temperature field of each micro ensemble. These additional micro ensemble runs are then integrated forward in time until 31 December 1999. Fischer et al. (2013) have shown that at the latest after a decade, the micro ensemble members exhibit a similar spread in atmospheric variables compared to members of the macro ensemble. Thus, for the period 1990–1999, the micro ensemble members can be regarded as additional independent members, yielding a total of 70 ensemble members covering the 10-year period from 1990–1999, i.e., 700 years of present-day climate. As for ERA-Interim data, a linear trend is removed from all JJA T2m data at each grid point and in each ensemble member. Note, however, that due to the ensemble set-up, this trend is calculated over only 10 years.

2.3 Decomposing a seasonal T2m anomaly to quantify the season's substructure

To examine the substructure of a particular July–August (JJA) season k, we decompose its seasonal T2m anomaly (SA_k) into contributions from the ranked D daily T2m values of season k, where D is the number of days in season k (e.g., for JJA $D = 92$). We thus aim to quantify how much each rank day (i.e., coldest day, second coldest day, etc.) of season k contributes to the seasonal anomaly SA_k. This decomposition of SA_k is illustrated for the example grid point 9°E/47°N (near Zürich, Switzerland) in Fig. 2 and introduced more formally below. It is applied to both data sets separately in exactly the same fashion and therefore, a superscript $M \in \{ERAI, CESM\}$ will only be used where it is necessary to explicitly distinguish between the two datasets. All the important statistical quantities used in this study are summarized in Tab. 1. Furthermore, bear in mind that all these quantities are calculated at each grid point individually.

We start by ranking all daily mean T2m values within their respective season k (Figs. 2a,b) and compute seasonal means (SM_k), i.e.,

$$SM_k = \frac{1}{D}\sum_{d=1}^{D} T_{d,k}, k = 1, \dots, K, \tag{1}$$

where $T_{d,k}$ is the daily mean T2m value with rank d in season k (i.e., the temporal ordering of the days is lost, see Fig. 2b). At each grid point we thus compute $K^{ERAI} = 40$ seasonal mean values for ERA-Interim and $K^{CESM} = 700$ values for CESM.

The climatological seasonal mean (C) is also calculated from the ranked daily mean T2m values ($T_{d,k}$) as

$$C = \frac{1}{K \cdot D}\sum_{k=1}^{K}\sum_{d=1}^{D} T_{d,k} = \frac{1}{D}\sum_{d=1}^{D}\frac{1}{K}\sum_{k=1}^{K} T_{d,k}\,. \tag{2}$$

Hereby, $\frac{1}{K}\sum_{k=1}^{K} T_{d,k}$ is the average T2m value of all K days with rank d in their respective season, e.g., for $d = 1$ the average coldest day of the season and for $d = 92$ the average hottest day of the season. Hence, C is computed as the mean over the average T2m values for each rank. These rank day T2m means (bold gray contour in Fig. 2b) are hereafter referred to as

$$RDM_d = \frac{1}{K}\sum_{k=1}^{K} T_{d,k}\,, d = 1, \dots, D. \tag{3}$$

Using the RDM_d, the seasonal T2m anomaly of any season k (SA_k) can be decomposed into contributions from each of the D rank days:

$$SA_k = SM_k - C = \frac{1}{D}\left(\sum_{d=1}^{D} T_{d,k} - \sum_{d=1}^{D} RDM_d\right) = \frac{1}{D}\sum_{d=1}^{D}(T_{d,k} - RDM_d) = \frac{1}{D}\sum_{d=1}^{D} RDA_{d,k}\,, \tag{4}$$

where in the last equality the rank day anomaly of the day with rank d in season k is introduced as $RDA_{d,k} = T_{d,k} - RDM_d$. In other words, the seasonal mean anomaly SA_k is expressed as the average rank day anomaly (see also Fig. 2c).

This decomposition of SA_k thus allows to assess the exact contribution from each (ranked) day of season k to SA_k. For example, if for a particular season k $SA_k = 1$ K and $RDA_{92,k} = 3$ K (i.e, the hottest day of season k is 3 K warmer than the respective rank day mean) this day contributed $3/92 = 0.0326$ K or 3.26% to the seasonal anomaly SA_k. In the following we split the 92 days of each JJA season k into three parts according to their rank and focus on the relative contributions to SA_k from the coldest, middle and hottest third of the 92 days of season k by calculating, e.g.,

$$SF_{cold,k} = \left(\frac{1}{D} \sum_{d=1}^{\left\lfloor \frac{D}{3} \right\rceil} RDA_{d,k} \right) \Big/ SA_k. \tag{5}$$

The notation $\lfloor x \rceil$ hereby stands for x rounded to the nearest integer. For computing contributions to SA_k from the middle and hottest thirds of the summer days ($SF_{middle,k}$ and $SF_{hot,k}$), the sum in Eq. (5) runs from $\left\lfloor \frac{D}{3} \right\rceil + 1$ to $\left\lfloor D\frac{2}{3} \right\rceil$ for $SF_{middle,k}$ and from $\left\lfloor D\frac{2}{3} \right\rceil + 1$ to D for $SF_{hot,k}$. By construction, the sum of the three fractions amounts to 1.

2.4 Identification and substructure of extreme summers

Extremely hot summers at each grid point in the Northern Hemisphere are identified in the ERA-Interim (CESM) data set as the 5 (35) hottest JJA seasons, yielding two sets of extreme summers $\mathbb{X}^M = \{k_1, \ldots, k_{N^M}\}, M \in \{ERAI, CESM\}$ with $N^{ERAI} = 5$ and $N^{CESM} = 35$ members, respectively. Hence, ERA-Interim extreme summers correspond to the 12.5% hottest summers (5 out of 40), while the CESM extreme summers correspond to the 5% hottest summers (35 out of 700).

An analogous procedure to that described in Sect. 2.3 is employed to quantify the contributions from each of the three thirds of the extreme summer days to the average T2m anomaly of the N considered extreme summers. The mean of these extreme summers (XM) is calculated as $XM = \frac{1}{N}\sum_{k\in\mathbb{X}} SM_k$ and is used to compute the mean anomaly of these extreme summers $XA = XM - C$. The relative contributions from the three thirds of the summer days to the extreme summer anomaly XA are calculated as, e.g.,

$$XF_{cold} = \left(\frac{1}{N} \sum_{k\in\mathbb{X}} \frac{1}{D} \sum_{d=1}^{\left\lfloor \frac{D}{3} \right\rceil} RDA_{d,k} \right) \Big/ XA. \tag{6}$$

The quantities XF_{cold}, XF_{middle} and XF_{hot} again add up to 1 and quantify the relative contributions from the three thirds to the average T2m anomaly of all extreme summers at a particular grid point. Note that the quantities XF_{cold}, XF_{middle} and XF_{hot} characterize the mean extreme summer substructure at a particular grid point, while $SF_{cold,k}$, $SF_{middle,k}$ and $SF_{hot,k}$ characterize the substructure of a single season k.

3 Results and discussion

3.1 Extreme summer T2m anomalies

Figures 3a and 4a depict the average T2m anomalies during extreme summers in the two data sets (XA^{ERAI} and XA^{CESM}, respectively). In both data sets, XA exhibits considerable spatial variability. The ERA-Interim extreme summers have temperature anomalies of up to 3 K over western Russia, while over some tropical ocean areas XA^{ERAI} is less than 0.5 K (Fig. 3a). The XA^{CESM} field exhibits a generally similar spatial pattern to XA^{ERAI}, with larger values over land than over the oceans (Fig. 4a). However, XA^{CESM} generally exceeds XA^{ERAI}, as the summers $\mathbb{X}^{CESM}$ are statistically more extreme than the summers $\mathbb{X}^{ERAI}$. In the following, we decompose the extreme summer T2m anomalies (XA) shown in Figs. 3a and 4a using the methodology described in Sect. 2.3 and 2.4, first at few selected grid points and then for all Northern Hemisphere grid points.

3.2 Extreme summer substructures at selected grid points

The rank day anomalies ($RDA_{d,k}^{ERAI}$) for the five ERA-Interim extreme summers at a grid point located in eastern India (81°E/21°N, Figs. 3a,b) reveal a similar substructure in at least four of the extreme summers. The largest $RDA_{d,k}^{ERAI}$ (up to 5 K) occur in the hottest 30 days of each season, while for the 60 coldest summer days in each extreme summer, $RDA_{d,k}^{ERAI}$ does not exceed 1.5 K. The contributions of the coldest, middle and hottest third of all extreme summer days to XA^{ERAI} at this grid point (i.e., XF_{cold}^{ERAI}, XF_{middle}^{ERAI} and XF_{hot}^{ERAI}) are 13%, 20% and 67%, respectively. For the 2005 summer, the contributions were -1%, 6% and 95%, and hence, almost the entire seasonal T2m anomaly resulted from the hottest 30 days of the summer being hotter than normal.

hat gelöscht: each
hat gelöscht: 10
hat gelöscht: 17
hat gelöscht: 73
hat gelöscht: 1
hat formatiert: Schriftfarbe: Text 1
hat formatiert: Schriftfarbe: Text 1
hat formatiert: Schriftfarbe: Text 1
hat gelöscht: 7
hat gelöscht: 92
hat gelöscht: ly

A comparison between the ERA-Interim and CESM extreme summer substructures at this grid point (Figs. 3b and 4b) reveals remarkable qualitative similarities between the extreme summer substructure at 81°E/21°N in the two data sets. At this grid point, also the season $\mathbb{X}^{CESM}$ exhibit largest $RDA_{d,k}^{CESM}$ values for the 30 hottest summer days. Moreover, despite the different number of seasons in the two data sets, the XF_{cold}^{CESM}, XF_{middle}^{CESM} and XF_{hot}^{CESM} values of 11%, 24% and 65%, respectively, are not far off the respective values for the seasons $\mathbb{X}^{ERAI}$. Figures 3b and 4b further reveal that the largest $RDA_{d,k}^{CESM}$ values reach much larger values (up to 8 K) than the $RDA_{d,k}^{ERAI}$ values, which is an expected result, since the seasons $\mathbb{X}^{CESM}$ are statistically more extreme than the seasons $\mathbb{X}^{ERAI}$.

hat gelöscht: 2
hat gelöscht: 3

Considering now the grid point 116°W/39°N in Nevada, USA, we find a substantially different ERA-Interim extreme summer substructure compared to eastern India (Figs. 3b,c), with largest extreme summer $RDA_{d,k}^{ERAI}$ values in the coldest third of the summer days and XF_{cold}^{ERAI}=49%, XF_{middle}^{ERAI}=31% and XF_{hot}^{ERAI}=20%. Also for this grid point, the mean substructure of CESM extreme summers is similar to that of ERA-Interim extreme summers, with XF_{cold}^{CESM}=42%, XF_{middle}^{CESM}=33% and XF_{hot}^{CESM}=25% (Fig. 4c). Thus, at this grid point, all thirds of the T2m distribution contribute to extreme summers, but the contribution from the coldest third is over proportionally large (i.e., considerably larger than 33%). Hence, the re-analysis and the climate model data both suggest that the suppression of cool summer days (leading to coldest days of the summer that are milder than usually) is a key ingredient for extreme summers at 116°W/39°N.

hat gelöscht: 44
hat gelöscht: 29
hat gelöscht: 27
hat gelöscht: 45
hat gelöscht: 31
hat gelöscht: 24

Yet a further extreme summer substructure is apparent at the grid point closest to Paris, France (2°E/49°N, Figs. 3d, 4d). At this grid point, the ERA-Interim extreme summer of 2018 was characterized by $RDA_{d,k}^{ERAI}$-values of 1.5–2 K for almost all ranks, i.e., this summer resulted from an almost uniform shift in the entire T2m distribution. Moreover, this grid point also illustrates that clearly distinct extreme summer substructures can occur at the same grid point. While the extreme summer 2003 exhibited particularly large anomalies in the coldest and the hottest third ($SF_{cold,2003}^{ERAI}$=34%, $SF_{middle,2003}^{ERAI}$=28% and $SF_{hot,2003}^{ERAI}$=38%), the contribution from the coldest third to the extreme summer 1995 was negative and the middle and top third were responsible for the entire seasonal anomaly ($SF_{cold,1995}^{ERAI}$=-15%, $SF_{middle,1995}^{ERAI}$=49% and $SF_{hot,1995}^{ERAI}$=66%, Fig. 3d).

Finally, the grid point 35°E/58°N in western Russia (Fig. 3e) illustrates that occasionally, the temperature variability during individual seasons can be fundamentally different from all other seasons at a particular grid point. Such a "regime shift" could be observed during the extreme summer 2010, which was characterized by $RDA_{d,2010}^{ERAI}$ values in excess of 4 K for ranks ~40–92 ($SF_{cold,2010}^{ERAI}$=1%, $SF_{middle,2010}^{ERAI}$=46% and $SF_{hot,2010}^{ERAI}$=53%). For these ranks, the $RDA_{d,2010}^{ERAI}$ values were almost twice as large as for the second hottest summer in these ranks (1981). The truly exceptional nature of the 2010 summer at 35°E/58°N (e.g., Barriopedro et al. 2011, Fig. 3e) becomes even more evident when comparing its $RDA_{d,k}^{ERAI}$ values with those of the CESM extreme summers at the same grid points (Figs. 4e). For some ranks, none of the 700 CESM JJA seasons reach $RDA_{d,k}^{CESM}$ values of comparable magnitude to those observed during the 2010 summer at this grid point. Some implications of this finding will be discussed in Sect. 4.

In summary, the mean extreme summer substructure at these four grid points is qualitatively remarkably similar for the 5 hottest ERA-Interim summers and the 35 hottest CESM summers. On the one hand, this similarity implies that the rank day anomaly patterns presented in Figs. 3b-e are not artefacts of the rather short ERA-Interim period, but rather must result from physical processes that shape the local extreme summer substructure. On the other hand, these similarities suggest that the CESM is able to correctly capture the processes that generate the distinct extreme summer substructures at these example grid points. We next compare the mean ERA-Interim and mean CESM extreme summer substructures at all grid points in the Northern Hemisphere by considering the spatial patterns of XF_{cold}^{ERAI}, XF_{hot}^{ERAI}, XF_{cold}^{CESM} and XF_{hot}^{CESM}.

3.3 Spatial variability of ERA-Interim and CESM extreme summer substructure

If extreme summers resulted from a uniform shift in the entire T2m distribution, all three thirds of the T2m distribution would contribute equally (i.e., 33%) to XA^{ERAI}. However, the XF_{hot}^{ERAI} field (Fig. 5a) reveals a complex pattern of coherent regions with increased (> 33%) or decreased (< 33%) contributions from the hottest third of extreme summer days to XA^{ERAI}. Land areas where particularly large XF_{hot}^{ERAI} values are found include the central US, the UK, parts of northeastern Europe, India and

hat gelöscht: Yet a further extreme summer substructure is apparent at the grid point closest to Munich, Germany (12°E/48°N, Figs. 3d, 4d). At this grid point, the ERA-Interim extreme summers of 2017 and 2018 were characterized by $RDA_{d,k}^{ERAI}$-values of 1.5–2.5 K for all ranks, i.e., these summers resulted from an almost uniform shift of approximately 2 K in the entire T2m distribution. ¶

hat gelöscht: ¶
Finally, the grid point 48°E/56°N in western Russia (Fig. 3e) illustrates that clearly distinct extreme summer substructures can occur at the same grid point. While the extreme summer 2013 exhibited largest $RDA_{d,2013}^{ERAI}$ values for relatively cool summer days ($SF_{cold,2013}^{ERAI}$=62%, $SF_{middle,2013}^{ERAI}$=28% and $SF_{hot,2013}^{ERAI}$=10%), the extreme summer 2010 was characterized by $RDA_{d,2010}^{ERAI}$ values in excess of 4 K for ranks ~40–92 ($SF_{cold,2010}^{ERAI}$=19%, $SF_{middle,2010}^{ERAI}$=35% and $SF_{hot,2010}^{ERAI}$=46%). The truly exceptional nature of the 2010 summer in Russia at 48°E/56°N (e.g., Barriopedro et al. 2011, Fig. 3e) and of the 2003 summer in Central Europe at 12°E/48°N (e.g., Stott et al. 2004, Fig. 3d) becomes particularly evident when comparing their $RDA_{d,k}^{ERAI}$ values with those of the CESM extreme summers at the same grid points (Figs. 4d,e). For some ranks, none of the 700 CESM JJA seasons reach $RDA_{d,k}^{CESM}$ values of comparable magnitude to those observed during the 2003 and 2010 summers at these two grid points. Some implications of this finding will be discussed in Sect. 4.¶

southeast Asia as well as the southern Sahel region (Fig. 5a). In some of these areas, $SF_{hot,k}^{ERAI}$ exceeded $SF_{middle,k}^{ERAI}$ and $SF_{cold,k}^{ERAI}$ during at least 4 out of 5 ERA-Interim extreme summers (stippling in Fig. 5a). In these regions, at least 4 out of 5 extreme summers thus exhibited a similar substructure. However, it is important to bear in mind that in other regions the substructure of individual extreme seasons (i.e., $SF_{cold,k}$, $SF_{middle,k}$ and $SF_{hot,k}$) may differ from the mean extreme season substructure characterized by XF_{cold}, XF_{middle} and XF_{hot}. Furthermore, also in parts of the northern North Pacific and northern North Atlantic, XF_{hot}^{ERAI} is substantially increased and reaches up to 60%. In many regions, however, XF_{hot}^{ERAI} is less than 33%, indicating that in these regions, extreme summers do not arise primarily from the hottest 30 days of the summer being hotter than climatologically.

In fact, in many regions it is the contribution to XA^{ERAI} from the coldest third of the summer (XF_{cold}^{ERAI}) that is substantially increased (Fig. 5c), for example the southwestern US, the northern Sahel region, Pakistan and parts of Greenland. Moreover, increased XF_{cold}^{ERAI} values are also found in the southern North Pacific and the southern North Atlantic as well as over the Arctic Ocean (Fig. 5c). Overall, Fig. 5c clearly demonstrates that the coldest third of all summer days contributes a substantial fraction to XA^{ERAI} in most regions [more than 25% over 83% of the Northern Hemisphere land area in ERAI]. In fact, in 46% of the Northern Hemisphere land area, XF_{cold}^{ERAI} exceeds XF_{hot}^{ERAI}, i.e., the coldest third of extreme summers contributes more to XA^{ERAI} than the hottest third. Consequently, in these regions the mechanisms that suppress unusually cool summer days must be considered when assessing the physical causes of extremely hot summers.

Comparing these results derived from ERAI with results based on CESM, i.e., XF_{hot}^{ERAI} and XF_{hot}^{CESM} (Figs. 5a,b) as well as XF_{cold}^{ERAI} and XF_{cold}^{CESM} (Figs. 5c,d), unravels strikingly similar patterns in many regions. For example, both data sets agree (even quantitatively) that extreme summers in India and Southeast Asia come about primarily by the hottest summer days being hotter than climatologically, while the coldest third of extreme summer days only contributes a marginal fraction to the respective XA. Also in the western and central US, XF_{cold} and XF_{hot} agree very well between the two data sets, with the cool summer days contributing an over proportionally large fraction to XA in the western US, and the hot summer days in the central US. Further areas of remarkable agreement between XF_{cold}^{ERAI} and XF_{cold}^{CESM} (Figs. 5c,d) are the high Arctic and the northern Sahel region. Moreover, in 49% of the Northern Hemisphere land area XF_{cold}^{CESM} exceeds XF_{hot}^{CESM}, which compares well with the 46% of the land area in which XF_{cold}^{ERAI} exceeds XF_{hot}^{ERAI}. Figure 5 thus clearly reveals that the CESM reproduces many features of the observed extreme summer substructure and its variability in space to a remarkable degree.

hat gelöscht: 50

However, there are also some areas of notable differences between XF_{hot}^{ERAI} and XF_{hot}^{CESM} as well as XF_{cold}^{ERAI} and XF_{cold}^{CESM}. For example over Greenland, Saudi Arabia and the northern North Atlantic, there are substantial differences between XF_{cold}^{ERAI} and XF_{cold}^{CESM} (Figs. 5c,d). Moreover, over the northern North Pacific as well as the high Arctic, the XF_{hot}^{CESM} and XF_{hot}^{ERAI} patterns agree only qualitatively, but not quantitatively (Figs. 5a,b). It is important to note, though, that some differences in the XF_{cold}

and XF_{hot} fields for the two data sets are expected due to the different sample sizes, even if the model was perfect. In the remainder of this paper we aim to explain statistical and physical reasons behind selected aspects of the spatial variability in XF_{cold} and XF_{hot}.

3.4 A statistical explanation for the observed extreme summer substructures

Figures 3b,c and 4b,c clearly illustrate that, at the selected grid points in India (81°E/21°N) and in the US (116°W/39°N) some rank days are climatologically much more variable than others. Importantly, this is the case not just for extreme summers but it is rather a climatological characteristic of the local temperature variability. For example, at 81°E/21°N the hottest 30 days of the summer are much more variable than the colder days. The 5th to 95th percentile range of the $RDA_{80,k}^{CESM}$-values is roughly four times larger than that of the $RDA_{10,k}^{CESM}$-values (Fig. 4b). At 116°W/39°N the largest rank day variability is found for lower ranks and the 5th to 95th percentile range of the $RDA_{80,k}^{CESM}$ values is roughly 2 times smaller than the same percentile range of the $RDA_{10,k}^{CESM}$-values (Fig. 4c). Similar ratios are found when comparing the spread of $RDA_{80,k}^{ERAI}$ and $RDA_{10,k}^{ERAI}$ for these two grid points (Figs. 3b,c). Moreover, at both grid points extreme summers occur when the most variable rank days are particularly hot (Figs. 3b,c and 4b,c). Hence, from a statistical point of view, the extreme summer substructure at these two particular grid points appears to be largely determined by the local "rank day variability pattern". That is, the contributions to XA from the distinct rank days during extreme summers depend on how variable the respective values $T_{d,k}$ are climatologically.

hat gelöscht: 5

We next assess whether the local rank day variability pattern also explains the extreme summer substructure at other Northern Hemisphere grid points. To do so, we consider the variance (V) of the $RDA_{d,k}$ values of all ranks and all JJA seasons at a particular grid point:

$$V = \frac{1}{K \cdot D} \sum_{k=1}^{K} \sum_{d=1}^{D} (RDA_{d,k})^2. \tag{7}$$

Here we have used the fact that the mean of the $RDA_{d,k}$ values is by construction equal to zero and thus their variance reduces to the average of the squared $RDA_{d,k}$-values of all d and all k. The contributions from the coldest, middle and hottest third to V are then e.g.,

$$VF_{cold} = \left(\frac{1}{K \cdot D} \sum_{k=1}^{K} \sum_{d=1}^{\left[\frac{D}{3}\right]} (RDA_{d,k})^2 \right) \Big/ V, \tag{8}$$

and analogously for the middle and hottest third of the summer days.

The fields of V^{ERAI} and V^{CESM} (Figs. 6a, 7a) resemble the XA^{ERAI} and XA^{CESM}-fields (Figs. 3a, 4a), as large rank day anomalies are a prerequisite for large seasonal T2m anomalies. Furthermore, comparing XF_{hot}^{ERAI} and VF_{hot}^{ERAI} (Figs. 5a and 6b) clearly reveals that wherever the contribution from the hottest third of the summer days to XA^{ERAI} is increased ($XF_{hot}^{ERAI} >$ 33%), the rank day variability in the hottest third (quantified by VF_{hot}^{ERAI}) contributes over proportionally to V^{ERAI}. Figures 5c and 6c illustrate that the same relationship also holds for XF_{cold}^{ERAI} and VF_{cold}^{ERAI}: regions where milder than normal cool summer days contribute over proportionally to XA^{ERAI} (i.e., $XF_{cold}^{ERAI} > 33\%$) exhibit increased VF_{cold}^{ERAI} values. Figures 5b,d and 7b,c confirm this finding also for the CESM data. We thus conclude that in both data sets, the extreme summer substructure is largely determined by the local rank day variability pattern.

hat gelöscht: closely

Furthermore, comparing the patterns of VF_{hot}^{ERAI} and VF_{hot}^{CESM} (Figs. 6b, 7b) reveals agreement in the same regions where also the patterns of XF_{hot}^{ERAI} and XF_{hot}^{CESM} (Figs. 5a,b) agree, and, conversely, disagreement between VF_{hot}^{ERAI} and VF_{hot}^{CESM} also results in disagreement between XF_{hot}^{ERAI} and XF_{hot}^{CESM}. For example, the VF_{hot}^{ERAI} and VF_{hot}^{CESM} fields (and the XF_{hot}^{ERAI} and XF_{hot}^{CESM} fields) are almost identical in India and Southeast Asia, the northern Sahel, the western US or Eastern Europe (cf. Figs. 6b and 7b, and Figs. 5a,b). Over Saudi Arabia or the northern North Atlantic, however, the patterns of VF_{hot}^{ERAI} and VF_{hot}^{CESM} (and of XF_{hot}^{ERAI} and XF_{hot}^{CESM}) do not agree particularly well. In summary, while the CESM correctly reproduces the local rank day variability pattern in most regions, differences in the local rank day variability patterns between the two data sets also lead to differences in the extreme summer substructures.

It is interesting to compare the VF_{cold} and VF_{hot} patterns presented in Figs. 6 and 7 with the skewness of the local daily temperature distributions, which has been studied extensively in the past (Donat and Alexander, 2012; Garfinkel and Harnik, 2017; Linz et al., 2018; Loikith et al., 2018; Loikith and Neelin, 2015; Ruff and Neelin, 2012). The upper tail of, e.g., a positively skewed JJA T2m distribution is longer than the lower tail, which is the case if the hottest summer days are more variable than the coldest summer (cf. Figs. 5b,c and Fig. S1). Hence, explanations of distinct skewness in daily T2m distributions also help to understand differences in the rank day variability patterns and, subsequently, extreme summer substructures. Garfinkel and Harnik (2017) showed that the winter low-level temperature distributions are positively skewed on the cold side of the Northern Hemisphere storm tracks, primarily because there the magnitude of warm air advection exceeds that of cold air advection. And, vice versa, the winter low-level temperature distributions are negatively skewed on the warm side of the Northern Hemisphere storm tracks, where the magnitude of cold air advection exceeds that of warm air advection. Consistent with their results, Figs. 6 and 7 depict more variable hot summer days to the north and more variable cold summer days to the south of the Northern Hemisphere storm tracks, where the horizontal gradients of T2m are particularly large (see in particular yellow contours in Figs. 6b,c).

hat gelöscht: days.

While this argument explains differences in the rank day variability and the extreme summer substructures in regions of strong surface temperature gradients, Figs. 5-7 also reveal numerous rather small-scale features, that do not necessarily occur in regions of strong surface temperature gradients. We therefore next analyze the extreme summer substructure and its causes in three example regions in more detail. Due to the similarity between the ERA-Interim and CESM extreme summer substructures, we restrict this analysis to ERA-Interim data (except where mentioned otherwise).

3.5 (Examples of) physical causes of extreme summer substructures

A particularly striking feature of Fig. 5 is the large contribution from the hottest third of the summer days to XA^{ERAI} in India, illustrated exemplarily for the grid point at 81°E/21°N in Fig. 3b. The general temperature evolution in JJA (i.e., considering all JJA seasons) at this grid point follows a particular sub-seasonal pattern (Fig. 8a). In early June, ERA-Interim T2m values are highly variable and range from 27°C to almost 40°C, with a mean of 35°C on 1 June. Throughout June and the first half of July the climatological T2m drops to approximately 26°C and remains at this level until the end of August. Moreover, during that period, the variability in T2m is much smaller than in early June. The extreme summers exhibit comparatively high temperatures primarily in June, while in July and August their T2m evolution does not differ substantially from other JJA seasons (Fig. 8a). The drop of T2m in June is associated with the onset of the Indian summer monsoon [Fig. 8b; e.g., Slingo, (1999)]. During most JJA seasons, precipitation starts to fall already during the first half of June. However, the extreme summers each featured very little precipitation for at least the first 20 days of June, which suggests that extreme summers at this grid point occur when there is an unusually late onset of the Indian summer monsoon at this particular location. Moreover, the rank day variability pattern at 81°E/21°N is easily understood from Fig. 8: The hottest days of the season mostly occur in June and are associated with dry conditions. The onset date of the monsoon determines how many dry (and thus very hot) days occur in a JJA season, i.e., an early onset of the Indian monsoon suppresses a large number of very hot days and a late onset increases this number, which leads to the large temperature variability seen in the warmest 30 days of the JJA season.

A further noteworthy feature in Fig. 5 is the sharp boundary in the extreme summer substructure around 75°N–80°N, for example in the North Atlantic sector. North of this boundary, the coldest third of all extreme summer days contribute up to 60% to the extreme summer anomaly (Figs. 5c,d). South of it, the contribution from the coldest third of extreme summer days is much smaller. (Quantitatively, there is some disagreement between the CESM and ERAI extreme summer substructures, but both data sets agree about the general pattern.) This sharp boundary in the extreme summer substructure is co-located with the climatological sea ice edge in JJA (Fig. 9a). Examining the JJA T2m distributions at three grid points across this boundary (42°W/83°N, 42°W/81°N and 42°W/79°N) reveals that for T2m below –1°C, their probability density functions (pdfs) of the daily T2m values are almost identical, which is not surprising due to their close spatial proximity. However, large differences in the three pdfs are found for T2m at about 0°C and above. At 83°N, i.e., north of the climatological sea ice edge (Fig. 9a), the pdf exhibits a very short upper tail with very little probability density exceeding +2°C (i.e., the pdf is strongly negatively skewed), while at 79°N (i.e., south of the climatological sea ice edge) the upper tail is much more variable. The geographical co-location of this extreme summer substructure boundary and of the climatological sea ice edge is striking and suggests that the contrasting substructures arise because the sea ice buffers "warm" temperatures at 0°C, that is, air with T2m > 0°C is cooled down to close to 0°C by the induced sea ice melting. The same effect has also been shown to shorten the upper tail of the surface temperature pdf over snow covered areas (Loikith et al., 2018).

As a third example, we return to the grid point in Nevada, US (at 116°W/39°N), where the rank day variability is largest for the cold summer days and extreme summers occur when the coldest 30 days exhibit mostly large positive rank day anomalies (Figs. 3c and 4c). Thus, at this grid point, milder than normal coldest days of the summer (or, equivalently, suppressed cool summer days) are a key ingredient for extreme summers. We therefore briefly explore why, at this grid point, the coldest summer days during extreme summers are warmer than normal.

hat gelöscht: ly

We first investigate what makes the climatologically coldest summer days at 116°W/39°N particularly cold and then contrast them with the coldest summer days during extreme summers at 116°W/39°N. A composite analysis of the upper-level flow during the 100 climatologically coldest ERA-Interim days of all 1979–2018 summers unravels a characteristic upper-level flow pattern: a highly amplified Rossby wave pattern over the eastern North Pacific and North America, with a breaking synoptic-scale trough covering 116°W/39°N (Fig. 10a). The breaking Rossby wave causing the trough is part of a synoptic-scale and transient wave packet (Fig. 10b) which has just the right phasing such that the trough axis crosses 116°W/39°N when the amplitude of the trough is largest (Fig. 10b). This type of relatively small-scale troughs, shown here with contours of potential vorticity on an isentrope in the upper troposphere (Fig. 10a), is relatively slow moving (Fig. 10b), such that the induced northwesterly low-level flow along its western flank can lead to strong and persistent cold-air advection to the western US. Additionally, the low-level flow induced by the trough impinges on the topography at the US west coast. Consequently, low-level air masses that are advected into the western US are most likely forced to ascend, which leads to adiabatic cooling of these already cool airmasses and finally results in the climatologically coldest summer days at 116°W/39°N.

The composites for the 100 coldest days during extreme summers, in contrast, do not reveal such a wave pattern (Figs. 10a and 10c). This indicates that the flow pattern characteristic of the climatologically coldest days at this grid point, i.e., the Rossby wave breaking and trough formation with the phasing discussed above, simply did not occur very often during extreme summers. Furthermore, a synoptic analysis of these 100 coldest extreme summer days (not shown) reveals that the associated upper-level flow configurations are rather variable, some featuring troughs while others even exhibited low-amplitude ridges, resulting in the rather zonal composite upper-level flow apparent in Figs. 10a and 10c.

Why in extreme summers at 116°W/39°N such highly amplified troughs with the right phasing did not occur is currently unclear, and at the same time challenging to assess. Possibly, the exact longitude where the synoptic-scale waves have been triggered (Röthlisberger et al., 2018) as well as the strength and longitudinal extent of the North Pacific jet, which modulates the waves' downstream propagation and breaking behavior (e.g., Drouard et al. 2015), might have played a role. However, both the jet strength and the characteristics of the transient waves propagating along the jet are strongly modulated by lower-frequency processes such as the Madden-Julian Oscillation (Moore et al., 2010) and the El Niño Southern Oscillation (Drouard et al., 2015; Shapiro et al., 2001). This example thus illustrates that a seamless approach, combining processes on different time scales, is most likely required to fully reveal the physical causes of extreme summers.

4 Summary and concluding remarks

In this study, extreme summers are defined in the upper tail of the JJA seasonal mean T2m distribution at each grid point in the Northern Hemisphere and then analyzed with regard to their substructure. Hereby, the extreme summer T2m anomaly is decomposed into its contribution from each rank day. First, all days are ranked within their respective season (i.e., from rank 1 to 92 for JJA) and then compared to the climatological T2m of all days with the same rank. The resulting rank day anomalies exactly quantify how much each (rank) day contributes to the T2m anomaly of the respective season and therefore allow for very intuitive statements about the characteristics of extreme summers. For example, we show that during the 2010 summer at the ERAI grid point at 35°E/58°N the 31 hottest days contributed 53% to the seasonal anomaly of 3.13 K and were each at least 4 K warmer than climatologically. This decomposition is applied to T2m data from ERA-Interim as well as data from 700 simulated years with CESM for present day climate conditions. Thereby, the contributions from the coldest, middle and hottest third of extreme summers to the extreme summer T2m anomalies are quantified at each Northern Hemisphere grid point (XF_{cold}, XF_{middle} and XF_{hot}).

This analysis reveals clearly distinct extreme summer substructures, occurring in coherent geographical regions. Despite the relatively small scale of the structures in the XF_{cold}^{ERAI} and XF_{hot}^{ERAI} fields as well as different numbers of extreme summers in the two data sets, CESM is able to reproduce these fields to a remarkable degree. This result firstly underlines that the ERA-Interim extreme summer substructures and their spatial variability result from physical processes rather than a too short data record and, secondly, testifies to the model's ability to reproduce the physical processes responsible for the occurrence of extreme summers in most regions in the Northern Hemisphere. Areas where CESM and ERA-Interim extreme summer substructures differ include Greenland, the northern North Atlantic as well as the Arabian Peninsula.

Furthermore, a key finding of this study is that the mean extreme summer substructure is consistent with the shape of the underlying local T2m distribution. The extreme summer substructure is largely determined by which of the 92 JJA rank days are most variable (i.e., the rank day variability pattern), which is qualitatively related to the skewness of the T2m distribution. Simply speaking, in regions where the coldest days of the summer are most variable (i.e., negatively skewed T2m distribution), extreme summers occur when the coldest days of the summer are unusually hot, and, analogously, for the case where hottest

hat gelöscht: we show that t

days vary the most (i.e., positively skewed T2m distribution). This finding is relevant for two reasons. Firstly, it constrains what kind of extreme summer substructures can locally be expected, in particular in regions with strongly skewed daily temperature distributions. For example, extreme summers arising primarily from extremely hot summer days (i.e., heat waves) are unlikely to occur in regions with strongly negatively skewed temperature distributions. Secondly, some individual extreme summers such as the 2010 summer at the grid point at 35°E/58°N featured clear temperature regime shifts, with rank day anomalies far outside of what could be expected from their climatological variability (e.g., almost twice as large as the second large anomalies for the same ranks during the 2010 summer at 35°E/58°N). The general consistency between the mean extreme summer substructure and the skewness of the underlying T2m distribution illustrates that such regime shifts in the temperature variability during extreme summers are the exception rather than the norm.

This consistency furthermore allows us to rely on previous work on physical causes of skewed surface temperature distributions for interpreting our results. Consistent with the findings of Garfinkel and Harnik (2017), we find distinct extreme summer substructures relative to the location of large surface temperature gradients, in particular in the Northern Hemisphere storm track regions. Extreme summers occurring north of the Northern Hemisphere storm tracks have large contributions from the hottest third of summer days, and south of the storm tracks the contributions from the coldest days are largest. This is primarily because on the cold side of a temperature gradient, warm air advection can reach much larger magnitudes than cold air advection, and vice versa on the warm side (e.g., Garfinkel and Harnik, 2017; Linz et al., 2018; Tamarin-Brodsky et al., 2019). Moreover, the few areas where the ERA-Interim and CESM extreme summer substructures differ, also have distinct rank day variability patterns in ERA-Interim and CESM. Thus, the climate model's ability to reproduce the ERA-Interim extreme summer substructures in most places results largely from the model's ability to produce local rank day variability patterns that agree with ERA-Interim.

However, three case studies illustrate that the extreme summer substructure cannot always be explained by temperature advection alone. In eastern India, more than 65% of the extreme summer T2m anomaly results from the hottest 30 days of JJA being hotter than climatologically. At the considered grid point, T2m exhibits a distinct sub-seasonal pattern, as it typically drops by almost 10 K with the onset of the Indian summer monsoon. Thus, the hottest days of the season (occurring in June) are highly variable, and extreme summers occur in seasons with particularly late monsoon onsets.

In the high Arctic the highest surface temperatures are buffered around 0°C, as excess heat would result in sea ice melting and subsequent latent cooling. Hence, the cold part of the T2m distribution accounts for most of the rank day anomaly variance and, consequently, extreme summers occur when the coldest summer days are warmer than normally. This buffering effect of the Arctic sea ice leads to a strong boundary in the extreme summer substructure around 75°N-80°N, i.e., near the climatological JJA sea ice edge.

hat nach unten verschoben [1]: Moreover, the few areas where the ERA-Interim and CESM extreme summer substructures differ, also have distinct rank day variability patterns in ERA-Interim and CESM. Thus, the climate model's ability to reproduce the ERA-Interim extreme summer substructures in most places results largely from the model's ability to produce local rank day variability patterns that agree with ERA-Interim.

hat gelöscht: . Moreover, the few areas where the ERA-Interim and CESM extreme summer substructures differ, also have distinct rank day variability patterns in ERA-Interim and CESM. Thus, the climate model's ability to reproduce the ERA-Interim extreme summer substructures in most places results largely from the model's ability to produce local rank day variability patterns that agree with ERA-Interim.

The rank day variability pattern is qualitatively related to the skewness of the T2m distribution: regions with positively (negatively) skewed T2m distributions exhibit larger variability in the upper (lower) ranks [e.g., compare Figs. 6 and 7 of this study with Fig. 4 in Loikith et al. (2018)]

hat gelöscht: Thus

hat gelöscht: ,

hat gelöscht: , we partly rely on previous work that investigated the physical causes of skewed surface temperature distributions

hat gelöscht:

hat gelöscht: (e.g., Garfinkel and Harnik, 2017)

hat verschoben (Einfügung) [1]

hat gelöscht:

hat gelöscht: often

hat gelöscht: 70

At a grid point in the western United States, all parts of the T2m distribution contribute significantly to extreme summers, however, an over proportionally large fraction comes from the coldest third of the extreme summer days (i.e., the coldest extreme summer days are warmer than their rank day mean). Composites of the upper-level flow during the 100 climatologically coldest summer days reveal that an amplified upper-level flow pattern with a particular phasing of a prominent trough and its associated cold air advection is characteristic of the climatologically coldest summer days at this grid point. This particular flow pattern did not occur frequently during the extreme summers, leading to milder than normal cool summer days. This result is consistent with previous work on physical causes of non-Gaussian temperature distributions (Garfinkel and Harnik, 2017; Linz et al., 2018; Tamarin-Brodsky et al., 2019), as it highlights the role of temperature advection by transient waves in generating a non-uniform rank day variability pattern, or similarly, a skewed T2m distribution.

Overall, the case studies illustrate that for understanding the physical causes of extreme summers, a seamless approach is necessary, which combines weather system dynamics, local thermodynamics and surface-atmosphere interactions as well as lower frequency variability in the atmosphere and the ocean. Clearly, distinct physical causes might lead to similar extreme summer substructures, in particular when comparing regions that are far apart (e.g., the northern Sahel region and the high Arctic, Fig. 5). However, similar extreme summer substructures in neighboring regions conceivably also point to similar physical causes of extreme summers (e.g., the Asian Monsoon region). Therefore, the extreme summer substructure is a helpful tool for discriminating between neighboring regions with distinct physical causes of extreme summers and might also be helpful for identifying coherent regions with similar physical causes of extreme summers.

hat gelöscht: The

hat gelöscht: hereby

hat gelöscht: identifying coherent

hat gelöscht: similar

A further key result of this study is that in most places, the cool summer days contribute substantially to extreme summer T2m anomalies [more than 25% over 83% (86%) of the Northern Hemisphere land area in ERAI (CESM)]. In fact, Fig. 5 reveals that for ERA-Interim (CESM) in 46% (49%) of the Northern Hemisphere land area, the coldest third of the summer contributes more to the extreme summer anomaly (XA) than the hottest third. Thus, large positive seasonal temperature anomalies (i.e. extreme summers as opposed to individual heat waves), cannot be understood and explained by only considering the physical drivers of heat waves. Rather, the processes which suppress the occurrence of cold summer days must also be considered. Yet, these processes are so far virtually unexplored and thus possibly yield an untapped potential for improving our understanding of extreme summers. However, as illustrated by the example of extreme summers in the western US, the processes that suppress the occurrence of cold summer days sometimes seem rather intangible, as they do not necessarily manifest themselves in the occurrence of an unusual flow pattern, but rather in the non-occurrence of the particular flow that typically produces the coldest summer days.

hat gelöscht: 50

hat gelöscht: whenever

hat gelöscht: are of interest

hat gelöscht: suppression

hat gelöscht: is fundamentally important

hat gelöscht: responsible

hat gelöscht: often

hat gelöscht: a

hat gelöscht: pattern rather than the occurrence of the flow pattern

This study has illustrated that extreme summers across the Northern Hemisphere have distinct substructures, which result directly from the physical causes of the extreme summers. However, the concept of the extreme season substructure has applications beyond what has been presented in this study and thus calls for subsequent studies. Firstly, the presented analyses could be extended to the Southern Hemisphere and other seasons and variables. (The application of the technique is most promising for variables that are potentially unbound and variable on both ends, i.e., not for a positive definite variable like precipitation.) Secondly, the concept of a "season substructure" can be relevant for field campaigns, as the representativeness of the campaigns' measurements depends on how representative the time period of the campaign was (Wernli et al., 2010). Thirdly, extreme summers with distinct substructures conceivably have different societal effects and thus future research should assess whether or not and where the extreme summer substructure is affected by climate change. The results of this study suggest that the CESM is a suitable tool for this task, as it is largely able to reproduce the observed (ERA-Interim) extreme summer substructure in the current climate. However, some of the extreme summers observed within the last 40 years appear to be outside of the spectrum of 700 years of CESM. Hence, while CESM is able to reproduce the local extreme summer substructures, it may not be able to reproduce the most extreme summers that are physically possible in some regions. Clearly, this finding requires detailed and critical further investigation. Finally, changes in the extreme summer substructure with climate change must be related to changes in the physical causes of extreme summers, as a uniform warming would not affect the local rank day variability pattern. Therefore, contrasting extreme summer substructures in present and future climate simulations might also help to identify regions where the physical causes of extreme summers are altered by climate change.

hat gelöscht: Secondly,

Data availability. ERA-Interim data can be downloaded from the ECMWF webpage (https://apps.ecmwf.int/datasets/data/interim-full-daily/levtype=sfc/). The CESM T2m data used here is available upon request from the authors.

Author contributions. MR and HW conceived the study, MS provided technical support, UB performed the CESM simulations, MR analyzed the data and wrote the major part of the manuscript. HW, EF, MS, and UB also contributed to writing the manuscript and commented on earlier versions of this manuscript.

Competing interests. The authors declare no conflict of interest.

Acknowledgements. MR, EF and HW acknowledge funding of the INTEXseas project from the European Research Council (ERC) under the European Union's Horizon 2020 research and innovation programme (grant agreement No 787652). Moreover, Maxi Boettcher (ETH Zürich) and Lukas Papritz (ETH Zürich) are acknowledged for helpful discussions during different stages of this work, Gary Strand (NCAR) and Clara Deser (NCAR) for providing the CESM restart files and two anonymous reviewers for providing thoughtful, challenging but yet encouraging reviews.

hat gelöscht: and

References

Barriopedro, D., Fischer, E., Luterbacher, J., Trigo, R. and Ricardo, G.-H.: The hot summer of 2010: Redrawing the temperature record map of Europe, Test, 332(6026), 220–224, doi:10.1126/science.1201224, 2011.

Brunner, L., Hegerl, G. C. and Steiner, A. K.: Connecting atmospheric blocking to European temperature extremes in spring, J. Clim., 30(2), 585–594, doi:10.1175/JCLI-D-16-0518.1, 2017.

Buras, A., Rammig, A. and Zang, C. S.: Quantifying impacts of the drought 2018 on European ecosystems in comparison to 2003, Biogeosciences Discuss., 1–23, doi:10.5194/bg-2019-286, 2019.

Ciais, P., Reichstein, M., Viovy, N., Granier, A., Ogée, J., Allard, V., Aubinet, M., Buchmann, N., Bernhofer, C., Carrara, A., Chevallier, F., De Noblet, N., Friend, A. D., Friedlingstein, P., Grünwald, T., Heinesch, B., Keronen, P., Knohl, A., Krinner, G., Loustau, D., Manca, G., Matteucci, G., Miglietta, F., Ourcival, J. M., Papale, D., Pilegaard, K., Rambal, S., Seufert, G., Soussana, J. F., Sanz, M. J., Schulze, E. D., Vesala, T. and Valentini, R.: Europe-wide reduction in primary productivity caused by the heat and drought in 2003, Nature, 437(7058), 529–533, doi:10.1038/nature03972, 2005.

Cohen, J., Screen, J. A., Furtado, J. C., Barlow, M., Whittleston, D., Coumou, D., Francis, J., Dethloff, K., Entekhabi, D., Overland, J. and Jones, J.: Recent Arctic amplification and extreme mid-latitude weather, Nat. Geosci., 7(9), 627–637, doi:10.1038/ngeo2234, 2014.

Dee, D. P., Uppala, S. M., Simmons, A. J., Berrisford, P., Poli, P., Kobayashi, S., Andrae, U., Balmaseda, M. A., Balsamo, G., Bauer, P., Bechtold, P., Beljaars, A. C. M., van de Berg, L., Bidlot, J., Bormann, N., Delsol, C., Dragani, R., Fuentes, M., Geer, A. J., Haimberger, L., Healy, S. B., Hersbach, H., Hólm, E. V., Isaksen, L., Kållberg, P., Köhler, M., Matricardi, M., Mcnally, A. P., Monge-Sanz, B. M., Morcrette, J.-J., Park, B.-K., Peubey, C., de Rosnay, P., Tavolato, C., Thépaut, J. N. and Vitart, F.: The ERA-Interim reanalysis: Configuration and performance of the data assimilation system, Q. J. R. Meteorol. Soc., 137(656), 553–597, doi:10.1002/qj.828, 2011.

Donat, M. G. and Alexander, L. V.: The shifting probability distribution of global daytime and night-time temperatures, Geophys. Res. Lett., 39(14), L14707, doi:10.1029/2012GL052459, 2012.

Dong, B., Sutton, R., Shaffrey, L. and Wilcox, L.: The 2015 European heat wave, Bull. Am. Meteorol. Soc., 97(12), 57–62, doi:10.1175/BAMS-D-16-0140.1, 2016.

Drouard, M., Rivière, G. and Arbogast, P.: The link between the North Pacific climate variability and the North Atlantic Oscillation via downstream propagation of synoptic waves, J. Clim., 28(10), 3957–3976, doi:10.1175/JCLI-D-14-00552.1, 2015.

Fink, A. H., Brücher, T., Krüger, A., Leckebusch, G. C., Pinto, J. G. and Ulbrich, U.: The 2003 European summer heatwaves and drought – synoptic diagnosis and impacts, Weather, 59(8), 209–216, doi:10.1256/wea.73.04, 2004.

Fischer, E. M., Seneviratne, S. I., Vidale, P. L., Lüthi, D. and Schär, C.: Soil moisture-atmosphere interactions during the 2003 European summer heat wave, J. Clim., 20(20), 5081–5099, doi:10.1175/JCLI4288.1, 2007.

Fischer, E. M., Beyerle, U. and Knutti, R.: Robust spatially aggregated projections of climate extremes, Nat. Clim. Chang.,

hat formatiert: Englisch (USA)

3(12), 1033–1038, doi:10.1038/nclimate2051, 2013.

Fouillet, A., Rey, G., Laurent, F., Pavillon, G., Bellec, S., Guihenneuc-Jouyaux, C., Clavel, J., Jougla, E. and Hémon, D.: Excess mortality related to the August 2003 heat wave in France, Int. Arch. Occup. Environ. Health, 80(1), 16–24, doi:10.1007/s00420-006-0089-4, 2006.

Garfinkel, C. I. and Harnik, N.: The non-Gaussianity and spatial asymmetry of temperature extremes relative to the storm track: The role of horizontal advection, J. Clim., 30(2), 445–464, doi:10.1175/JCLI-D-15-0806.1, 2017.

Hoskins, B.: The potential for skill across the range of the seamless weather-climate prediction problem: A stimulus for our science, Q. J. R. Meteorol. Soc., 139(672), 573–584, doi:10.1002/qj.1991, 2013.

Hoy, A., Hänsel, S., Skalak, P., Ustrnul, Z. and Bochníček, O.: The extreme European summer of 2015 in a long-term perspective, Int. J. Climatol., 37(2), 943–962, doi:10.1002/joc.4751, 2017.

Hurrell, J. W., Holland, M. M., Gent, P. R., Ghan, S., Kay, J. E., Kushner, P. J., Lamarque, J.-F., Large, W. G., Lawrence, D., Lindsay, K., Lipscomb, W. H., Long, M. C., Mahowald, N., Marsh, D. R., Neale, R. B., Rasch, P., Vavrus, S., Vertenstein, M., Bader, D., Collins, W. D., Hack, J. J., Kiehl, J., Marshall, S., Hurrell, J. W., Holland, M. M., Gent, P. R., Ghan, S., Kay, J. E., Kushner, P. J., Lamarque, J.-F., Large, W. G., Lawrence, D., Lindsay, K., Lipscomb, W. H., Long, M. C., Mahowald, N., Marsh, D. R., Neale, R. B., Rasch, P., Vavrus, S., Vertenstein, M., Bader, D., Collins, W. D., Hack, J. J., Kiehl, J. and Marshall, S.: The Community Earth System Model: A framework for collaborative research, Bull. Am. Meteorol. Soc., 94(9), 1339–1360, doi:10.1175/BAMS-D-12-00121.1, 2013.

Kay, J. E., Deser, C., Phillips, A., Mai, A., Hannay, C., Strand, G., Arblaster, J. M., Bates, S. C., Danabasoglu, G., Edwards, J., Holland, M., Kushner, P., Lamarque, J.-F., Lawrence, D., Lindsay, K., Middleton, A., Munoz, E., Neale, R., Oleson, K., Polvani, L., Vertenstein, M., Kay, J. E., Deser, C., Phillips, A., Mai, A., Hannay, C., Strand, G., Arblaster, J. M., Bates, S. C., Danabasoglu, G., Edwards, J., Holland, M., Kushner, P., Lamarque, J.-F., Lawrence, D., Lindsay, K., Middleton, A., Munoz, E., Neale, R., Oleson, K., Polvani, L. and Vertenstein, M.: The Community Earth System Model (CESM) Large Ensemble Project: A community resource for studying climate change in the presence of internal climate variability, Bull. Am. Meteorol. Soc., 96(8), 1333–1349, doi:10.1175/BAMS-D-13-00255.1, 2015.

Linz, M., Chen, G. and Hu, Z.: Large-scale atmospheric control on non-Gaussian tails of midlatitude temperature distributions, Geophys. Res. Lett., 45(17), 9141–9149, doi:10.1029/2018GL079324, 2018.

Loikith, P. C. and Neelin, J. D.: Short-tailed temperature distributions over North America and implications for future changes in extremes, Geophys. Res. Lett., 42(20), 8577–8585, doi:10.1002/2015GL065602, 2015.

Loikith, P. C., Neelin, J. D., Meyerson, J. and Hunter, J. S.: Short warm-side temperature distribution tails drive hot spots of warm temperature extreme increases under near-future warming, J. Clim., 31(23), 9469–9487, doi:10.1175/JCLI-D-17-0878.1, 2018.

Lorenz, R., Jaeger, E. B. and Seneviratne, S. I.: Persistence of heat waves and its link to soil moisture memory, Geophys. Res. Lett., 37(L09703), doi:10.1029/2010GL042764, 2010.

Moore, R. W., Martius, O. and Spengler, T.: The modulation of the subtropical and extratropical atmosphere in the Pacific basin in response to the Madden–Julian oscillation, Mon. Weather Rev., 138(7), 2761–2779, doi:10.1175/2010MWR3194.1, 2010.

Orth, R., Zscheischler, J. and Seneviratne, S. I.: Record dry summer in 2015 challenges precipitation projections in Central Europe, Sci. Rep., 6(1), 28334, doi:10.1038/srep28334, 2016.

Pfahl, S. and Wernli, H.: Quantifying the relevance of atmospheric blocking for co-located temperature extremes in the Northern Hemisphere on (sub-)daily time scales, Geophys. Res. Lett., 39(12), 1–6, doi:10.1029/2012GL052261, 2012.

Röthlisberger, M. and Martius, O.: Quantifying the local effect of Northern Hemisphere atmospheric blocks on the persistence of summer hot and dry spells, Geophys. Res. Lett., 46(16), 10101–10111, doi:10.1029/2019GL083745, 2019.

Röthlisberger, M., Martius, O. and Wernli, H.: Northern Hemisphere Rossby wave initiation events on the extratropical jet–A climatological analysis, J. Clim., 31(2), 743–760, doi:10.1175/JCLI-D-17-0346.1, 2018.

Röthlisberger, M., Frossard, L., Bosart, L. F., Keyser, D. and Martius, O.: Recurrent synoptic-scale Rossby wave patterns and their effect on the persistence of cold and hot spells, J. Clim., 32, 3207–3226, doi:10.1175/JCLI-D-18-0664.1, 2019.

Ruff, T. W. and Neelin, J. D.: Long tails in regional surface temperature probability distributions with implications for extremes under global warming, Geophys. Res. Lett., 39(4), L04704, doi:10.1029/2011GL050610, 2012.

Russo, S., Sillmann, J. and Fischer, E. M.: Top ten European heatwaves since 1950 and their occurrence in the coming decades, Environ. Res. Lett., 10(12), 124003, doi:10.1088/1748-9326/10/12/124003, 2015.

Schär, C. and Jendritzky, G.: Hot news from summer 2003, Nature, 432(7017), 559–560, doi:10.1038/432559a, 2004.

Schneidereit, A., Schubert, S., Vargin, P., Lunkeit, F., Zhu, X., Peters, D. H. W. and Fraedrich, K.: Large-scale flow and the long-lasting blocking high over Russia: Summer 2010, Mon. Weather Rev., 140(9), 2967–2981, doi:10.1175/MWR-D-11-00249.1, 2012.

Seneviratne, S. I., Corti, T., Davin, E. L., Hirschi, M., Jaeger, E. B., Lehner, I., Orlowsky, B. and Teuling, A. J.: Investigating soil moisture-climate interactions in a changing climate: A review, Earth-Science Rev., 99(3–4), 125–161, doi:10.1016/j.earscirev.2010.02.004, 2010.

Shapiro, M. A., Wernli, H., Bond, N. A. and Langland, R.: The influence of the 1997–99 El Niño Southern Oscillation on extratropical baroclinic life cycles over the eastern North Pacific, Q. J. R. Meteorol. Soc., 127(572), 331–342, doi:10.1002/qj.49712757205, 2001.

Slingo, J.: The Indian summer monsoon and its variability, in Beyond El Niño: Decadal and interdecadal climate variability, edited by A. Navarra, pp. 103–116, Springer, Berlin., 1999.

Sousa, P. M., Trigo, R. M., Barriopedro, D., Soares, P. M. M. and Santos, J. A.: European temperature responses to blocking and ridge regional patterns, Clim. Dyn., 50(1–2), 457–477, doi:10.1007/s00382-017-3620-2, 2018.

Tamarin-Brodsky, T., Hodges, K., Hoskins, B. J. and Shepherd, T. G.: A dynamical perspective on atmospheric temperature variability and its response to climate change, J. Clim., 32(6), 1707–1724, doi:10.1175/JCLI-D-18-0462.1, 2019.

Vogel, M. M., Zscheischler, J., Wartenburger, R., Dee, D. and Seneviratne, S. I.: Concurrent 2018 hot extremes across Northern Hemisphere due to human-induced climate change, Earth's Futur., 7(7), 2019EF001189, doi:10.1029/2019EF001189, 2019.

Wehner, M., Stone, D., Krishnan, H., AchutaRao, K. and Castillo, F.: The deadly combination of heat and humidity in India and Pakistan in summer 2015, Bull. Am. Meteorol. Soc., 97(12), 81–86, doi:10.1175/BAMS-D-16-0145.1, 2016.

Wernli, H., Pfahl, S., Trentmann, J. and Zimmer, M.: How representative were the meteorological conditions during the COPS field experiment in summer 2007?, Meteorol. Zeitschrift, 19(6), 619–630, doi:10.1127/0941-2948/2010/0483, 2010.

Zschenderlein, P., Fink, A. H., Pfahl, S. and Wernli, H.: Processes determining heat waves across different European climates, Q. J. R. Meteorol. Soc., qj.3599, doi:10.1002/qj.3599, 2019.

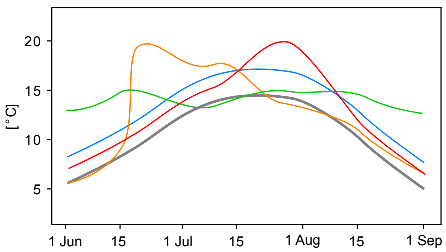

Figure 1. Schematic surface temperature evolution during extreme summers with different substructures: an extreme summer arising from just one heat wave (orange), from a suppression of cool summer days (green) and from a shift in the entire T2m distribution (blue) and from a general shift towards higher temperatures and a heat wave (red). The schematic climatological surface temperature evolution is depicted in gray.

hat gelöscht: , from two heat waves

hat gelöscht: with a rather cool period separating the two heat waves (red),…

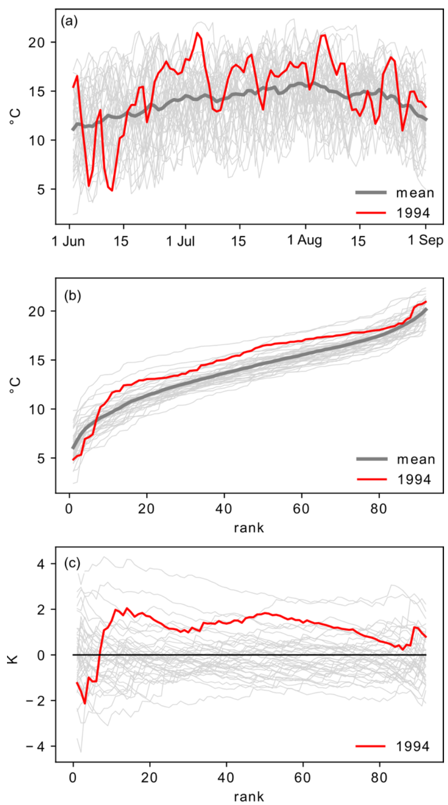

Figure 2. Steps in computing $\boldsymbol{RDA_{d,k}^{ERAI}}$-values at the grid point closest to Zürich, Switzerland (9°E/47°N). Values for the 1994 summer are highlighted in red. Panel (a) shows ERA-Interim T2m at 9°E/47°N for all 40 ERA-Interim summers. The sorted T2m values ($\boldsymbol{T_{d,k}^{ERAI}}$) are shown in panel (b) and the $\boldsymbol{RDA_{d,k}^{ERAI}}$-values in panel (c). Note that for illustrating purposes Fig. 2 presents non-detrended T2m data.

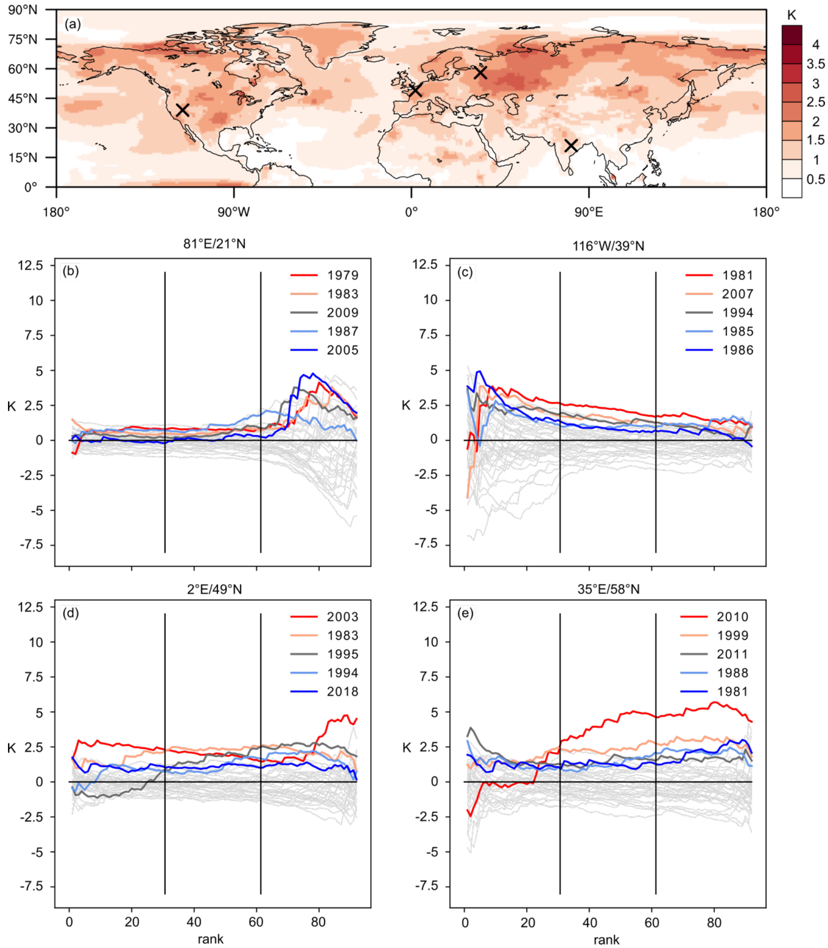

Figure 3. Extreme summer T2m anomaly and extreme summer substructure for selected grid points in ERA-Interim. Panel (a) depicts $\boldsymbol{XA}^{\boldsymbol{ERAI}}$, panels (b–e) show $\boldsymbol{RDA}_{\boldsymbol{d,k}}^{\boldsymbol{ERAI}}$ for the five ERA-Interim extreme summers in colours and for the remaining summers in light grey. Crosses in panel (a) indicate the grid points for which the $\boldsymbol{RDA}_{\boldsymbol{d,k}}^{\boldsymbol{ERAI}}$-values are shown in panels (b–e).

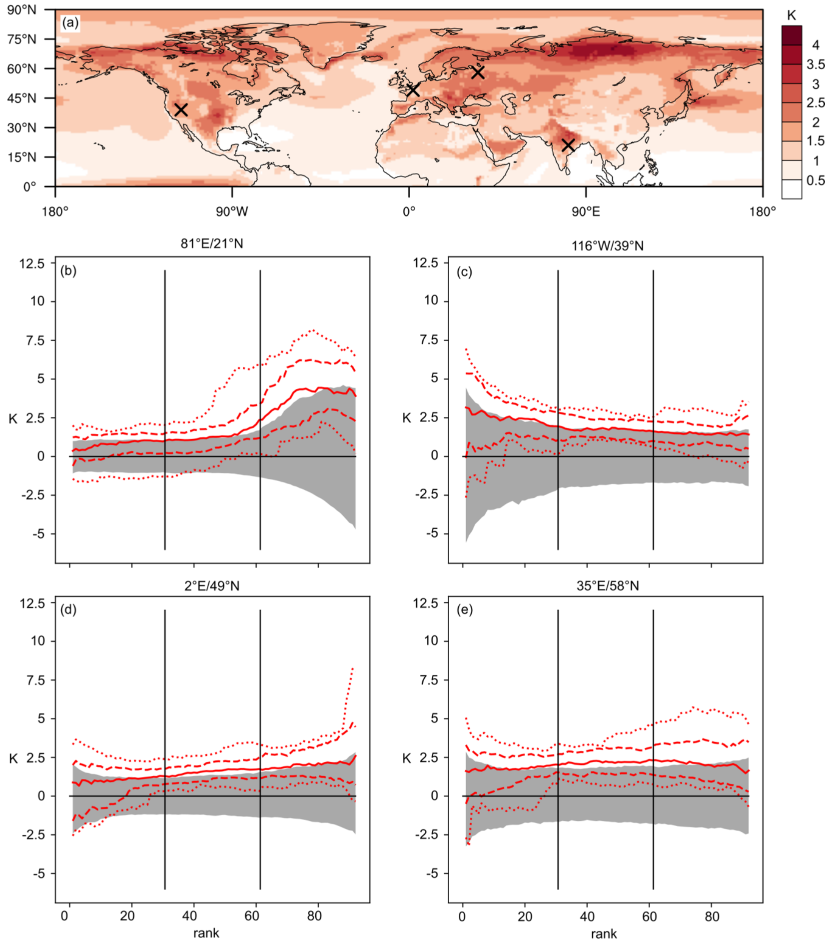

Figure 4. Extreme summer T2m anomaly and extreme summer substructure for selected grid points in CESM. Panel (a) displays XA^{CESM} and panels (b–e) show in red the maximum and minimum (dotted), 90th and 10th percentile (dashed) and the median (solid red) $RDA_{d,k}^{CESM}$ of the 35 CESM extreme summers. The 5th to 95th percentile range of the $RDA_{d,k}^{CESM}$ of all JJA seasons are depicted in grey. Crosses in panel (a) indicate the grid points for which the rank day anomalies are shown in panels (b–e).

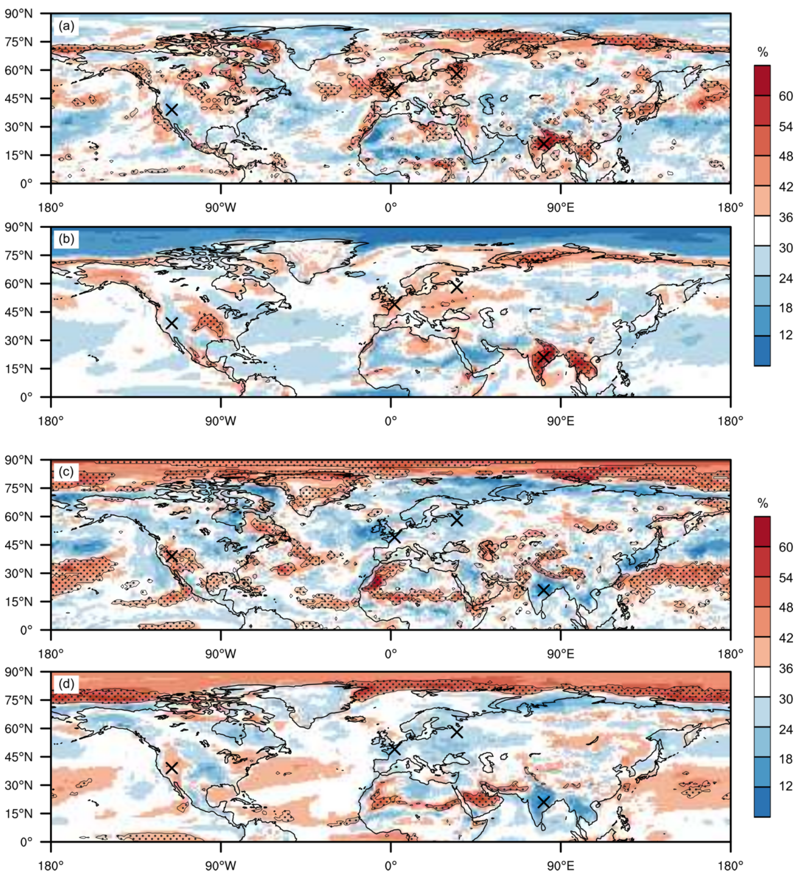

Figure 5. Spatial variability in the extreme summer substructure in ERA-Interim and CESM. Panels (a) and (b) depict XF_{hot}^{ERAI} and XF_{hot}^{CESM}, respectively, while XF_{cold}^{ERAI} and XF_{cold}^{CESM} are shown in panels (c) and (d). Stippled areas in all panels indicate grid points at which the same third of the distribution contributes the largest fraction of all thirds to at least 80% of the extreme summers (i.e., similar substructure in at least 80% of the extreme summers). Black crosses as in Fig. 3a.

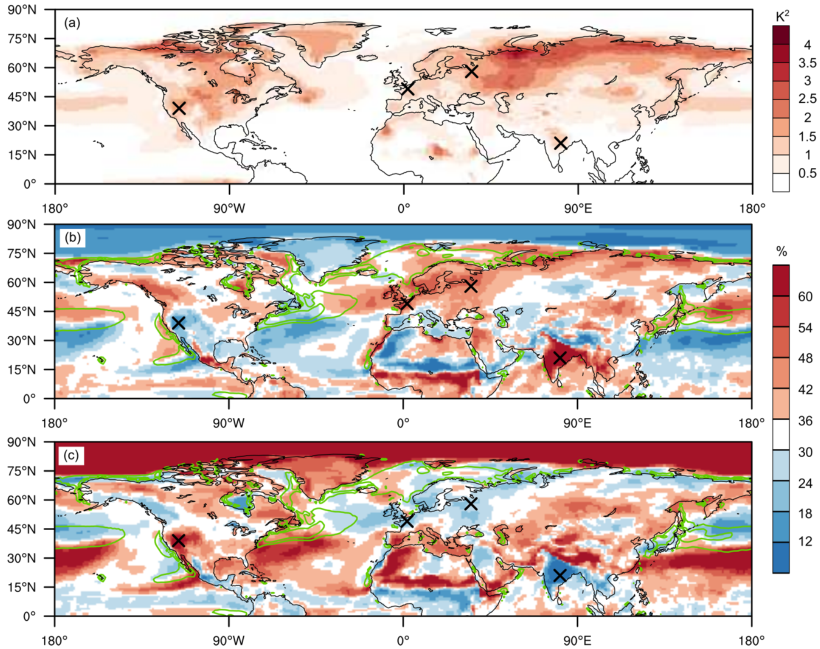

Figure 6. The variance of $\boldsymbol{RDA_{d,k}^{ERAI}}$ and its contributions from the coldest and hottest third of summer days. Panel (a) depicts $\boldsymbol{V^{ERAI}}$ and panels (b) and (c) show $\boldsymbol{VF_{hot}^{ERAI}}$ and $\boldsymbol{VF_{cold}^{ERAI}}$, respectively. Yellow contours in (b) and (c) depict $\boldsymbol{C^{ERAI}}$ gradient magnitudes of 6 and 12 K 10^{-6} m^{-1}. The $\boldsymbol{C^{ERAI}}$ gradient magnitudes have been computed as first order central differences and are only plotted over oceans. Black crosses as in Fig. 3a.

hat gelöscht: 5, 10

hat gelöscht: 15

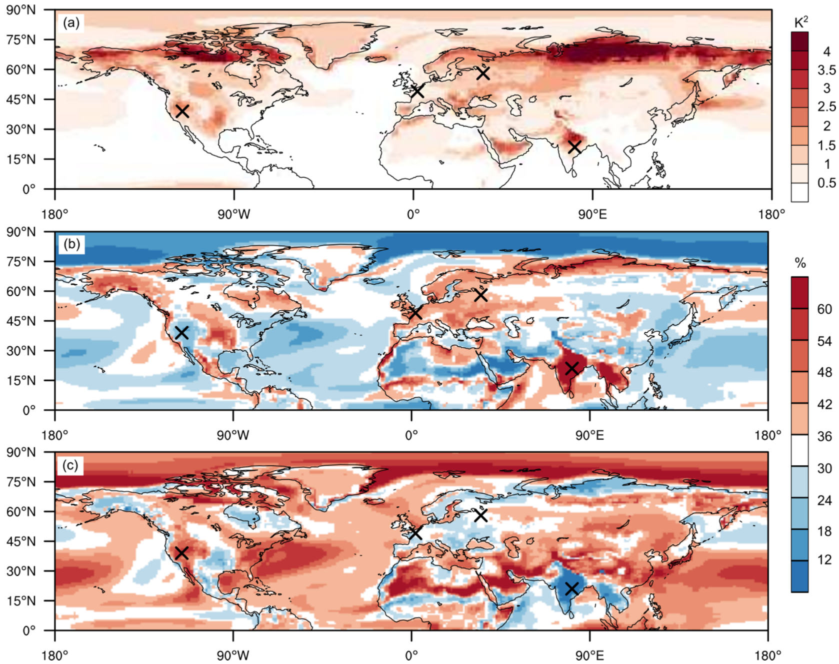

Figure 7. The variance of $\boldsymbol{RDA_{d,k}^{CESM}}$ and its contributions from the coldest and hottest third of summer days. Panel (a) depicts $\boldsymbol{V^{CESM}}$ and panels (b) and (c) show $\boldsymbol{VF_{hot}^{CESM}}$ and $\boldsymbol{VF_{cold}^{CESM}}$, respectively. Black crosses as in Fig. 3a.

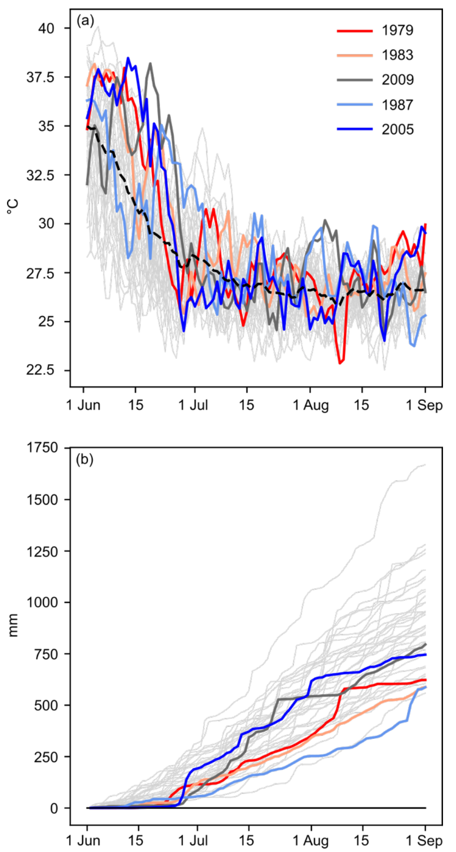

Figure 8. The JJA temperature and precipitation evolution at 81°E/21°N. Panels (a) and (b) depict non-detrended ERA-Interim T2m and accumulated precipitation at 81°E/21°N for all JJA seasons, respectively. The extreme summers are highlighted in colors. The dashed black line in (a) depicts the climatological calendar day mean T2m at 81°E/21°N.

hat formatiert: Schriftart: Nicht Fett

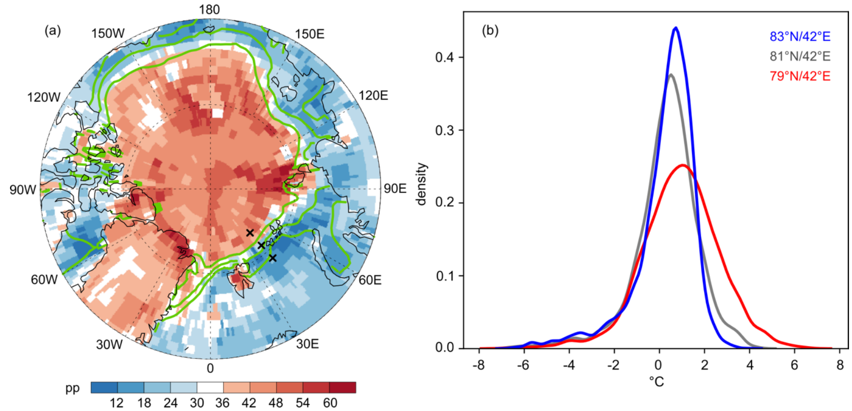

Figure 9. Arctic sea ice and local summer temperature variability. Panel (a): $\boldsymbol{XF_{cold}^{ERAI}}$ (shading, only 70°N–90°N is shown) and mean 1979–2018 JJA ERA-Interim sea ice concentration (yellow contours indicate sea ice concentrations of 0.3, 0.5 and 0.7). Panel (b): empirical probability density function of non-detrended ERA-Interim T2m at 79°N/42°E (red), 81°N/42°E (gray) and 83°N/42°E (blue). Crosses in (a) locate these three grid points.

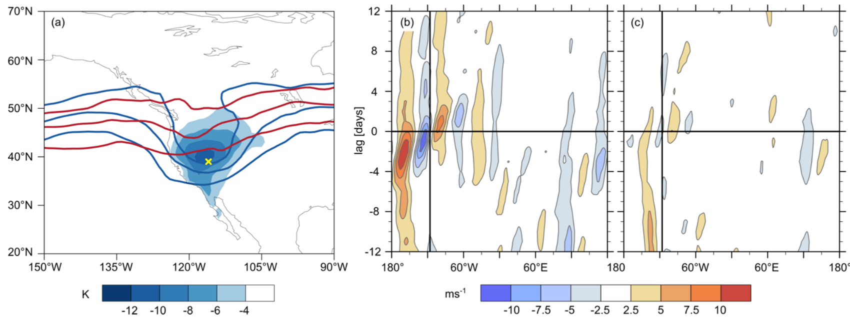

Figure 10. (a) T2m difference between the 100 climatologically coldest JJA days and the 100 coldest extreme summer days (shading). Contours depict the composite PV field at 335 K (contours of 2, 3.5 and 5 PVU) for the 100 climatologically coldest JJA days (blue) and for the 100 coldest extreme summer days (red). The yellow cross indicates 116°W/39°N. Panels (b) and (c) depict composite Hovmöller diagrams of the anomalous 250 hPa meridional wind, averaged between 35°N and 65°N temporally centered on the 100 climatologically coldest JJA days (b) and on the 100 coldest extreme summer days (c). Meridional wind anomalies are calculated relative to the 1979–2018 mean JJA meridional wind. The vertical line in (b) and (c) indicates 116°W.

Table 1. Definitions and descriptions of important quantities used in this study.

Symbol	Formal definition	Description
$T_{d,k}$		Daily mean T2m with rank d in season k (Fig. 2b)
SM_k	$\frac{1}{D}\sum_{d=1}^{D} T_{d,k}$	Seasonal mean T2m of season k
C	$\frac{1}{K \cdot D}\sum_{k=1}^{K}\sum_{d=1}^{D} T_{d,k}$	Climatological JJA seasonal mean
SA_k	$SM_k - C$	Seasonal anomaly of season k
RDM_d	$\frac{1}{K}\sum_{k=1}^{K} T_{d,k}$	Rank day mean of rank d
$RDA_{d,k}$	$T_{d,k} - RDM_d$	Rank day anomaly of rank d in season k (Figs. 2c, 3b–e, 4b–e)
XM	$\frac{1}{N}\sum_{k \in X} SM_k$	Mean of N considered extreme summers
XA	$XM - C$	Mean anomaly of N considered extreme summers (Figs. 3a, 4a)
$SF_{cold,k}$	$\left(\frac{1}{D}\sum_{d=1}^{\left[\frac{D}{3}\right]} RDA_{d,k}\right) \Big/ SA_k$	Fractional contribution from the coldest third of summer days of season k to SA_k
XF_{cold}	$\left(\frac{1}{N}\sum_{k \in X}\frac{1}{D}\sum_{d=1}^{\left[\frac{D}{3}\right]} RDA_{d,k}\right) \Big/ XA$	Fractional contribution from coldest third of extreme summer days to XA (Fig. 5)
V	$\frac{1}{K \cdot D}\sum_{k=1}^{K}\sum_{d=1}^{D} (RDA_{d,k})^2$	Variance of all $RDA_{d,k}$ values at a particular grid point. (Figs. 6a, 7a)
VF_{cold}	$\left(\frac{1}{K \cdot D}\sum_{k=1}^{K}\sum_{d=1}^{\left[\frac{D}{3}\right]} (RDA_{d,k})^2\right) \Big/ V$	Fractional contribution from the coldest third of all summer days to V (Figs. 6b,c, 7b,c)

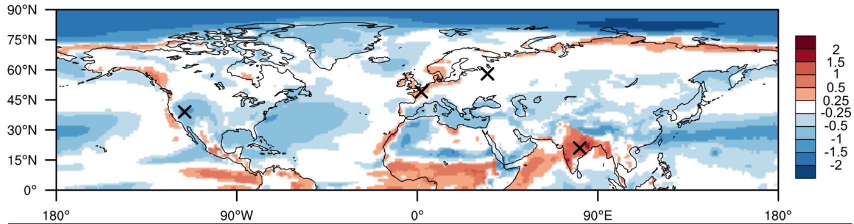

Figure S1. Skewness of daily T2m in ERA-Interim. Black crosses as in Fig. 3a.